ELSEVIER

Marine Chemistry 57 (1997) 137–161

MARINE CHEMISTRY

Marine Chemistry Discussion Paper

What controls dissolved iron concentrations in the world ocean?

Kenneth S. Johnson [a,b,*], R. Michael Gordon [a], Kenneth H. Coale [a]

[a] *Moss Landing Marine Laboratories, P.O. Box 450, Moss Landing, CA 95039, USA*
[b] *Monterey Bay Aquarium Research Institute, P.O. Box 628, Moss Landing, CA 95039, USA*

Accepted 8 April 1997

Abstract

Dissolved (< 0.4 μm) iron has been measured in 354 samples at 30 stations in the North and South Pacific, Southern Ocean and North Atlantic by the Trace Metals Laboratory at Moss Landing Marine Laboratories. These stations are all more than 50 km from a continental margin. The global distribution of dissolved iron, which is derived from these profiles, is remarkable for several reasons. The dissolved iron profiles have a uniform shape with a nutrient-like profile at each station. Concentrations at the surface are all < 0.2 nmol kg^{-1} and average 0.07 nmol kg^{-1}. Below 500 m, the average concentration is 0.76 nmol kg^{-1}. The largest value in the data set is 1.38 nmol kg^{-1}. There is no inter-ocean fractionation, which is unique for an element with a nutrient-like profile. Published estimates of the iron residence time are on the order of 100 to 200 yr, indicative of rapid removal. Other elements with such short residence times are characterized by vertical profiles that decrease with depth and deep concentrations that decrease with age as water passes from the Atlantic to the Pacific. This is not the case for iron. The largest horizontal changes in dissolved iron are observed in gradients from the continental margin. There is only a factor of three difference between the minimum (0.4 nmol kg^{-1}) and maximum (1.3 nmol kg^{-1}) value in the data set at a depth near 750 m, where variability is at a maximum. The minimum concentrations are found at stations in the remote central Pacific and the maximum values occur at stations adjacent to the continental margin. The major source of iron in the deep sea is generally aeolian deposition. Integrated (surface to 500 m) concentrations of iron at each station are only weakly correlated with the aeolian iron deposition flux, however. This contrasts with other elements such as lead that also have strong atmospheric sources. These observations lead us to conclude that the nutrient-like profile is maintained by a mechanism that reduces the scavenging rate of dissolved iron at concentrations less than 0.6 nmol kg^{-1}. This mechanism may be complexation by strong iron binding ligands, which have been found in both the Atlantic and Pacific at concentrations near 0.6 nM. This apparent solubility would act to diminish inter-ocean fractionation. It would allow a nutrient-like profile to develop before scavenging began to remove iron. In order to test the concept, we developed a numerical model to make quantitative predictions of dissolved iron concentrations from place to place. The dissolved iron source in the ocean interior is remineralization from sinking particulate organic matter. Scavenging removes dissolved iron only at concentrations greater than the apparent solubility. The only geographically variable parameter in the model is the export flux of carbon from the surface layer, which carries iron with it. The model generated dissolved iron profiles, based on measured or estimated values of the carbon export flux, are in remarkable agreement with the observed profiles at all stations from the North Atlantic through the Southern Ocean to the North Pacific. © 1997 Elsevier Science B.V.

* Corresponding author.

PII S0304-4203(97)00043-1

1. Introduction

There is considerable interest in the biogeochemical cycling of iron (Bruland et al., 1991; Geider and La Roche, 1994; de Baar, 1994; Wells et al., 1995; Hutchins, 1995). The role of iron in controlling oceanic productivity in high nitrate low chlorophyll (HNLC) waters has been clearly demonstrated. Experiments by several groups have shown that iron will increase phytoplankton growth rates when it is added to containers of HNLC seawater, if sufficient care is taken not to contaminate the control samples with iron (Martin and Fitzwater, 1988; Martin et al., 1989, 1990a; Coale, 1991; Johnson et al., 1994; de Baar et al., 1990). These effects have been demonstrated in HNLC waters of the subarctic Pacific, equatorial Pacific, and the Southern Ocean. Three deliberate iron addition experiments in the equatorial Pacific show dramatic increases in phytoplankton growth after iron is added (Martin et al., 1994; Coale et al., 1996b). These effects are clear at added dissolved iron concentrations of 0.3 nmol kg^{-1}, just 4 to 5 times greater than the ambient concentration. Paleoceanographic tracers of ocean productivity show a strong correlation between export of carbon and iron accumulation rates in sediments of the Southern Ocean (Kumar et al., 1995). Observations of chlorophyll following dust deposition events suggest a strong linkage between dust input and primary production (Young et al., 1991).

Despite this interest in the role of iron in regulating primary production, there have been no comprehensive assessments of the processes that control iron concentrations in the ocean. The trace metals laboratory at Moss Landing Marine Laboratories has collected and reported a series of profiles for dissolved and particulate iron concentrations in waters throughout the world ocean (Martin and Gordon, 1988; Martin et al., 1989, 1990b, 1993; Coale et al., 1996a). These data show that the vertical profile of iron is nutrient-like, with low concentrations in the surface layer and increasing concentrations with depth. The concentrations of iron are closely correlated with that of nitrate in the subarctic North Pacific (Martin et al., 1989), as one might expect for a limiting nutrient.

The oceanic distribution of iron is not completely nutrient-like, however. Iron does not show a strong inter-ocean fractionation (Martin et al., 1993), in contrast to nitrate. Other micro-nutrient metals, such as zinc, show clear differences between the Atlantic and Pacific (Bruland and Franks, 1983). One might expect that if iron is remineralized from sinking biogenic debris and accumulated in the water column, as iron appears to be in the subarctic North Pacific (Martin et al., 1989), then its concentration should be much lower in the Atlantic. Nutrient elements also generally have oceanic residence times longer than that of water in the ocean, on the order of $10^3 < \tau < 10^5$ yr (Whitfield and Turner, 1987). For example, phosphate has a residence time of approximately 7×10^4 yr (Broecker and Peng, 1982). Estimates of the dissolved iron residence time in seawater are much shorter than the thermohaline circulation time (1000 yr). Bruland et al. (1994) estimate the residence time of iron in the deep-sea to be 70 to 140 yr, while Landing and Bruland (1987) estimated values of 58 yr over the depth range 0 to 1400 m. It is difficult to imagine how an element with a residence time < 200 yr could accumulate a nutrient-like profile in less than one ocean mixing cycle in all regions of the ocean. In fact, elements with residence times less than one ocean mixing cycle typically show a depletion in the Pacific, relative to the Atlantic (Whitfield and Turner, 1987), as do manganese (Bruland and Franks, 1983) and aluminum (Orians and Bruland, 1985). The simple surface water uptake and deep-water remineralization cycle that is typical of other elements with nutrient-like profiles is insufficient to describe the distribution of iron.

These observations suggest that many of the processes controlling iron distributions are unique. One might be tempted to suggest that these observations imply that there is a significant error in the measurement of dissolved iron. As we show below, there is good agreement between our results and those obtained by other laboratories with proven capabilities for ultra-trace metal analysis in the ocean. In this paper, we focus primarily on the MLML data set for iron for several reasons. First, these data are analytically consistent. There are no reference standards for iron at oceanic concentrations (< 1 nM). It is difficult to account for interlaboratory differences in iron measurements, therefore, unless repeated occupations of the same oceanic area have been made by

different laboratories. The iron profiles in the MLML data set also show smooth changes with depth that correlate with other oceanographic features. Finally, the MLML data set encompasses most regions of the open ocean, with the notable exception of the South Atlantic, Indian and Arctic Oceans.

In our recent work, we have attempted to quantify the processes controlling metal distributions by placing our studies within the framework of numerical models (Johnson et al., 1994, 1996; Gordon et al., submitted). In order to assess whether the mechanisms that we consider here are consistent with known oceanographic processes, we present a simple model for iron cycling. This model incorporates the processes that we believe are most likely to control dissolved iron concentrations. This model quantitatively accounts for the distribution of iron that we have observed throughout the world ocean. The quantitatively defensible predictions that it generates are strong evidence that the model accurately represents the major features of the oceanic iron cycle.

2. Data set

The complete data set for dissolved and particulate iron concentrations is available on the MLML home page on the World Wide Web at the address http://color.mlml.calstate.edu/www/data/. The primary data set consists of 30 open ocean concentration profiles. Fig. 1 shows the locations of the vertical profiles in the open ocean. Many of the profiles are reported here for the first time, while some of the data has been described in previous publications (Martin and Gordon, 1988; Martin et al., 1989, 1990a,b, 1993; Coale et al., 1996a; Gordon et al., submitted). All of the sample collection and analyses were performed using the same procedures. In every case, samples were collected using Teflon coated 30 l Go-Flo bottles suspended on non-metallic Kevlar line and tripped with Teflon messengers. Only 2 bottles were used per cast because our clean van is only equipped to filter two samples at a time. This minimized the time that each sample was in the

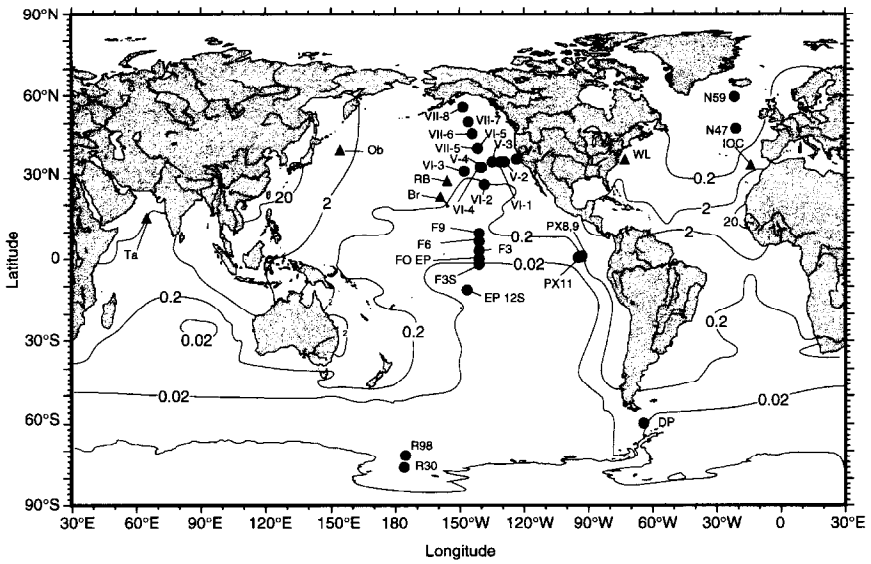

Fig. 1. Station locations where the MLML Trace Metals Laboratory has measured iron (solid circles) and where other laboratories have also measured consistent concentrations of dissolved iron (solid triangles). Also shown on the map are contours of aeolian iron flux to the sea surface (from Duce and Tindale, 1991). Contour intervals in units of mg m^{-2} yr^{-1} reported by Duce and Tindale (1991) were converted to μmol m^{-2} yr^{-1} by assuming an atomic weight of 50 for iron. The labels for the triangles refer to the data source (Br-Bruland et al., 1994; RB-Rue and Bruland, 1995; WL-Wu and Luther (1994); IOC-Landing et al., 1995; Ob-Obata et al., 1993; Ta-Takeda et al., 1995). The labels for the circles refer to the MLML Trace Metals lab station designation: Roman numerals refer to VERTEX cruise number and station, F refers to FeLine stations, EP to JGOFS EqPac stations, PX to PlumEx stations, R to Ross Sea stations, DP to Drake Passage stations and N to JGOFS NABE stations.

bottle. As a result, each complete profile required two to three days for collection. The Go-Flo bottles were acid cleaned prior to each cruise and they remained covered with plastic bags at all times except during deployment and recovery operations. Water was drained through a Teflon stopcock with an internal Teflon tube extension that reached to the bottom of the bottle, allowing filtration of all sample water. Go-Flo bottles were pressurized to 0.5 bar with filtered nitrogen gas and the sample water passed into the MLML trace metal clean van through polyethylene tubing. Inside the clean van, sample water was filtered through tared, acid-washed Nuclepore polycarbonate membrane filters (142 mm, 0.4 μm) mounted in Teflon sandwiches.

Two aliquots of the filtrate were collected in separate, acid-cleaned, low density polyethylene bottles and acidified to pH < 2 with 4 ml of 6 N quartz distilled hydrochloric acid (QHCl) per liter. Dissolved iron was operationally defined as the fraction which passed through the 0.4 μm filter. Dissolved iron was preconcentrated in Teflon separatory funnels using 1% APDC-DDDC liquid–liquid organic extraction into chloroform (Bruland et al., 1979). The technique consisted of a double forward extraction without a back extraction step in order to minimize blank values. The chloroform containing the extracted iron was evaporated in quartz beakers and digested with several aliquots of quartz distilled nitric acid ($QHNO_3$).

The polycarbonate filters containing the particulate iron were sequentially digested with 6 N QHCl, concentrated $QHNO_3$, and Ultrex (J.T. Baker) hydrofluoric acid. Digestion took place in an all Teflon bomb which was heated in a boiling water bath for a total of 3 h (Eggiman and Betzer, 1976).

All water collection, filtration and sample preparation was performed in MLML trace metal clean rooms using all plastic laminar flow hoods and clean benches of Class 100 or better. All analyses were conducted using a Perkin-Elmer Zeeman 5000 atomic absorption spectrophotometer coupled to an HGA 500 graphite furnace.

Detection limits for dissolved iron were based on a 250 ml sample and twice the standard deviation of the mean blank level. The variability in blank analyses has decreased somewhat over the time period involved in this study (1984 to present). Absolute blank levels have also decreased to generally less than 0.02 total nanomoles of iron in the concentrated extracts. Values reported are averages of two extractions from two separate sample aliquots unless one sample was contaminated.

Of the 398 samples collected and analyzed for dissolved iron on the cruises discussed here, 44 samples were believed to be contaminated and are not included. The contamination almost always appeared to be associated with the Go-Flo bottles (both replicates were high) and not the polyethylene sample collection bottles or analysis. Contaminated samples typically represented isolated outliers that occurred randomly in the data sets. However, every other sample from the Drake Passage profile was contaminated (7 samples total) because they were all collected with the same defective Go-Flo bottle (Martin et al., 1990b).

The remaining 354 samples in the open ocean data set will be the primary focus of this paper. This set of 354 samples includes only those collected more than 50 km from a continental land mass. We will also consider profiles of iron concentrations determined closer to the continental margin, and which have been previously reported (Martin and Gordon, 1988; Martin et al., 1989, 1990a,b), when we discuss horizontal gradients. The profiles from the Ross Sea and the PlumEx experiment near the Galapagos Islands represent only a subset of the data that we have collected in these regions. The remainder of the Ross Sea data will be discussed in another publication (Fitzwater et al., in preparation). The remainder of the PlumEx data is discussed fully by Gordon et al. (submitted).

3. Overview of the MLML data set

3.1. Dissolved iron

Fig. 2a shows the concentrations of dissolved iron plotted versus depth for all 30 stations in the MLML data set that are > 50 km from a continental land mass. Mixed layer concentrations are all less than 0.2 nmol kg^{-1}. Dissolved iron increases with depth below the mixed layer at each station and all profiles converge on values in the range 0.5 to 0.9 nmol kg^{-1} at depths below 1700 m. The concentrations

reach maximum values of 1 to 1.3 nmol kg^{-1} in profiles located near the coast. The maximum occurs at depths between 500 and 1000 m and then concentrations decrease at greater depth until they converge with the central gyre profiles. There is only a factor of three difference between the minimum (0.4 nmol kg^{-1}) and maximum (1.3 nmol kg^{-1}) value in the data set at a depth near 750 m. As discussed below, there are strong gradients near the coast. If the 4 stations nearest the coast in the North Pacific (VERTEX V-1, V-2, VI-1, VII-8) are excluded, then the uniformity of the open ocean profiles is even more evident (Fig. 2b).

The results reported here for the open ocean come primarily from the North Pacific. There are also two profiles from the North Atlantic, three profiles in the Pacific sector of the Southern Ocean (including the Drake Passage) and two in the tropical South Pacific. All of these profiles are generally consistent with the results seen in the North Pacific (Fig. 2). Together, these regions account for roughly 60% of the total ocean volume. The uniformity of the iron concentrations within this fraction of the ocean suggests that most of the remaining volume that lies more than 50 km from the coast, and which has not yet been sampled (primarily the South Atlantic, Indian and Arctic Ocean), should also have iron concentrations typical of those summarized here. The average of all of the measurements of iron at distances of more than 50 km from the coast is 0.38 nmol kg^{-1} ($n = 354$). In the mixed layer, dissolved iron concentrations are all < 0.2 nmol kg^{-1} with an average of 0.07 ± 0.04 nmol kg^{-1} ($n = 112$). The average is skewed in the high direction because many of the observations are reported as the detection limit. The average iron concentration at depths below 500 m is 0.76 ± 0.25 nmol kg^{-1} ($n = 117$).

We believe that these profiles are an accurate representation of dissolved iron concentrations in the bulk of the ocean for two reasons. First, as we discuss below, the profiles are consistent with oceanographic processes, in the sense used by Boyle et al. (1977). We develop a model based on simple oceanographic principles to test the consistency of the measurements. The model quantitatively describes the differences in iron concentrations from site to site based on known changes in oceanographic properties. Second, there is compelling agreement between these data and results generated by others with extensive trace metal experience at open ocean levels. Dissolved iron profiles in the central North Pacific (Bruland et al., 1994; Rue and Bruland, 1995), in the western North Atlantic (Wu and Luther, 1994), and in the western North Pacific

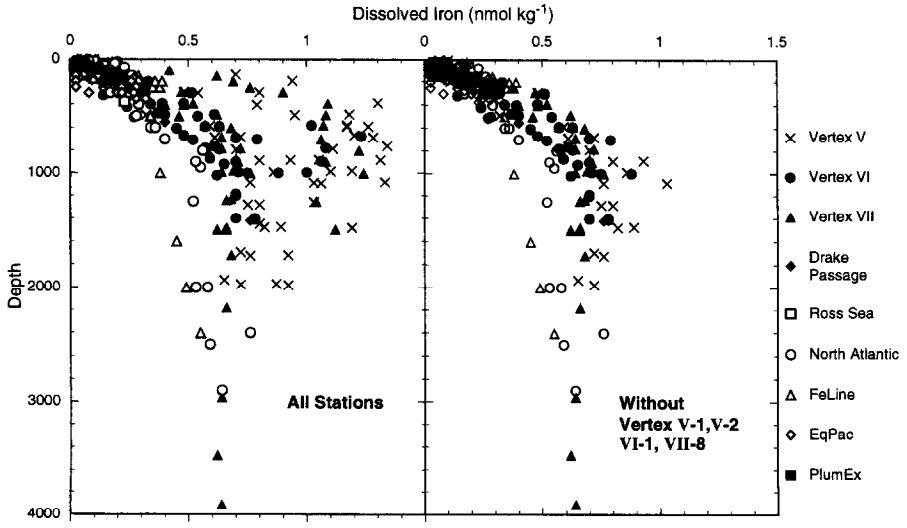

Fig. 2. (A) Dissolved (< 0.4 μm) iron concentrations measured in 354 samples at stations more than 50 km from the continental coastline. (B) Dissolved (< 0.4) iron concentrations as in (A), but excluding the 4 stations closest to shore (VERTEX V-1, V-2, VI-1, VII-8) in the North Pacific.

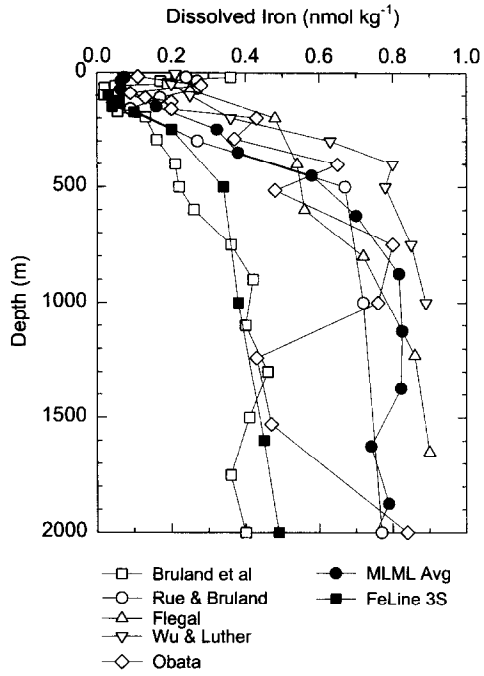

Fig. 3. Comparison of the MLML results with dissolved iron measurements obtained by Bruland et al. (1994), Rue and Bruland (1995), Flegal/UCSC in the IOC intercalibration (Landing et al., 1995), Wu and Luther (1994) and Obata et al. (1993). The average profile calculated from all of the MLML data in Fig. 2 is shown, as is the single profile determined at 3°S, 140°W on the FeLine cruise.

(Obata et al., 1993) are quite similar to the results that we have found (Fig. 3). These data sets all follow relatively smooth trends. The single profile of iron that follows a smooth trend versus depth (Flegal, UCSC) in the IOC trace metal intercalibration exercise (Landing et al., 1995) is also substantially similar to the results that we have obtained (Fig. 3). This station was located in the eastern North Atlantic. The iron profile reported by Landing in the IOC exercise is also similar to the data we find, except for a series of high values from 500 to 1200 m. In addition, an iron profile in the Arabian Sea reported by Takeda et al. (1995) has quite low values in the upper 100 m, above the extremely strong oxygen minimum layer found in this area.

There are many iron profiles reported in the literature that consist of iron concentrations substantially different than the results that we have obtained. The dissolved iron concentrations in these other studies are higher than the results that have been determined by the MLML Trace Metals Laboratory, which may be indicative of contamination during sampling and analysis. We believe that it is imperative to resolve these differences in the future by establishing iron in seawater standards with concentrations that span the range found in the data set reported here. In addition, an intercalibration that involves each laboratory using its usual sample collection procedures must be conducted. In the mean time, there is sufficient interlaboratory agreement and oceanographic consistency with the MLML data set to make a convincing argument that it is typical of most of the ocean. Observations of anomalous dissolved iron concentrations, such as high values at the surface (> 0.5 nmol kg^{-1}), should be accompanied by a suite of observations that reproduce the nutrient-like iron profiles shown in Figs. 2 and 3. This will add confidence that anomalous values are not analytical artifacts.

3.2. Particulate iron

Particulate iron was measured at only a subset of the stations discussed here. Most of the samples from the remaining stations are archived, but have not been analyzed due to financial constraints. The particulate iron data set spans a somewhat larger concentration range than does the dissolved iron data set (Fig. 4). The concentrations of particulate iron reach values near 5 nmol kg^{-1}. Concentrations greater than 1 nmol kg^{-1} are limited to 4 stations near the continental margin. These are VERTEX V, Stations 1 and 2 near the California margin, VERTEX VII, Station 8 near the Alaska margin and Station 30 over the continental slope in the Ross Sea. The particulate iron concentrations are all < 1 nmol kg^{-1} at the remaining stations, with the exception of 1 sample.

The particulate iron concentrations in the North Pacific are generally similar to the values reported by Bruland et al. (1994), if the 4 stations near the continental margin are excluded. Concentrations of particulate iron at the surface are typically within the range of 0.1 to 0.3 nmol kg^{-1}, while Bruland et al. report concentrations from 0.1 to 0.2 nmol kg^{-1}. The concentrations increase with depth at most stations. Deep water (> 1000 m) concentrations of particulate iron are in the range of 0.2 to 0.8 nmol kg^{-1}, which encompasses the range of values (0.2 to

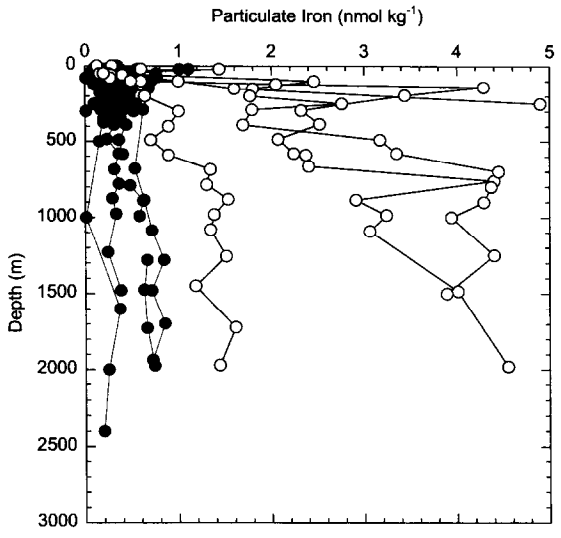

Fig. 4. Vertical profiles of particulate (> 0.4 μm) iron. Data at four stations near the continental margin are shown as open circles (VERTEX V, Stations 1 and 2 near the California margin, VERTEX VII, Station 8 near the Alaska margin and Station 30 over the continental slope in the Ross Sea). The remaining stations are shown as closed circles.

0.4 nmol kg^{-1}) reported by Bruland et al. (1994) at depths below 1000 m. The particulate iron profile that we observed at the FeLine 3°S station, which has the dissolved iron profile most similar to that reported by Bruland et al. (1994), also has a very similar particulate iron profile.

4. Processes regulating dissolved iron concentrations

4.1. Offshore gradients

The horizontal variability in the dissolved iron data is associated with gradients from high concentrations near shore to low values in the open ocean. High dissolved iron concentrations (> 0.2 nmol kg^{-1}) in the mixed layer over the continental shelf and slope decay to concentrations < 0.2 nmol kg^{-1} in waters more than 50 km offshore at locations in the North Pacific (Martin and Gordon, 1988) and in the Ross Sea (e.g., Fig. 5). The scale length for dissolved iron transport, defined as the distance over which concentrations drop to 1/e of the initial value, was estimated by plotting ln[(Fe)] from a near surface transect in Monterey Bay versus the distance from shore (Fig. 6). The slope of this plot is −0.062 km^{-1}, which corresponds to a scale length (1/slope) of 16 km. Over a distance of 4 scale lengths (64 km), the dissolved iron concentrations would be reduced to about 2% ($e^{-0.062 * 64} = 0.019$) of the concentration adjacent to the coast (Fig. 6). The mixed layer concentrations at distances 50 to 100 km from the continental margins are less than 0.15 nmol kg^{-1} and they are indistinguishable from open ocean iron concentrations. These data suggest that high coastal iron concentrations do not penetrate far into the surface ocean. Near-shore regions have the potential to be iron limited (see below).

A meridional section near 140°W from the Alaska Margin (55°N) to 15°S and a zonal section of dissolved iron near 30°N from 122°W near the California coast to 147°W are shown in Fig. 7a, b. These sections were constructed from all of the available dissolved iron data in the MLML data set along these lines that are more than 50 km from the shelf break. Surface iron concentrations are very low along both sections. The 0.2 nmol kg^{-1} contour is located well below 100 m, except near the coast, in both sections. As in the surface, high iron concentrations near the coast are apparent at all depths below the mixed layer. These high iron concentrations extend 1000 km offshore at depths below 500 m. Thus, the

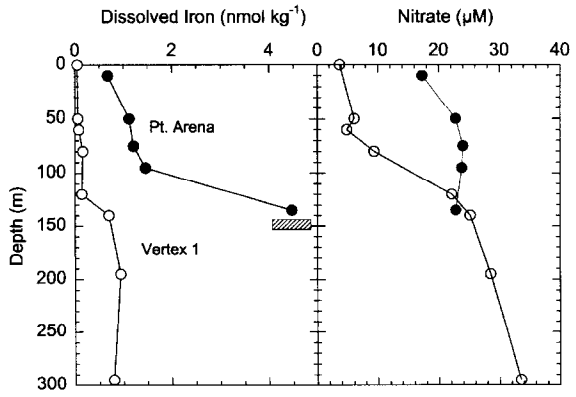

Fig. 5. Profiles of dissolved iron (a, left) and nitrate (b, right) measured at VERTEX V, Station 1 located 75 km off the California coast and at ONR Station (11) located 10 km off the open California coast. Data from Martin and Gordon (1988).

scale length for decay of the offshore dissolved iron gradient within the main thermocline is much longer than at the surface. The slope of a plot of ln[(Fe)] at 1000 m versus distance from shore along the zonal section is -0.0002 km^{-1} (Fig. 6). This slope is equivalent to a scale length of 5000 km to reduce dissolved iron concentrations to 37% (1/e) of the initial concentration. Note that very high iron concentrations (>4 nmol kg^{-1}) observed at depths down to 800 m near the bottom at stations over the continental slope (Martin and Gordon, 1988; Martin et al., 1989) are not observed at any of the open ocean stations. The scale length for transport of these very high iron concentrations must be considerably shorter than 1000 m.

The scale length for iron penetration offshore at depths near 1000 m is several times greater to the west, off California, than it is in the southerly direction off the coast of Alaska (Fig. 7: note the horizontal scale difference in a and b). The large scale length for iron transport to the west appears to be limited to a narrow band of latitudes centered near 30°N (Fig. 7a). Dissolved iron concentrations drop rapidly to the north and south of 30°N at all depths below 800 m along 140°W. This may be related to the filaments of water that cross the California Current (Bernstein et al., 1977), transporting chemicals far offshore.

4.2. Relationship of iron to oxygen and recycled nutrients

The increasing concentration of iron with depth suggests that it is involved in a particle remineralization cycle similar to nutrients such as nitrate (Martin and Gordon, 1988; Sunda and Huntsman, 1995). If we plot iron versus apparent oxygen utilization (AOU) for stations in the North Atlantic and North Pacific, however, we see quite different results (Fig. 8). In the North Pacific, iron increases with AOU. Nearly the same increase in iron occurs in the North Atlantic, but there is a much smaller increase in AOU. Dissolved Fe and AOU remain highly correlated in the North Atlantic, but the slope of the relationship is much greater. In the South Equatorial Pacific, AOU increases rapidly with depth through the shallow (200 m) oxygen minimum, while iron remains <0.1 nmol kg^{-1} through the core of the oxygen minimum. Iron increases below this depth in the South Equatorial Pacific, while AOU does not change much. As a result, dissolved iron and AOU are very poorly correlated at this station.

If we compare iron profiles to those of nitrate, an element that is highly correlated with AOU, we see quite a difference in behavior (Fig. 9). Each iron profile is qualitatively similar to the corresponding nitrate profile. There is significant inter-ocean frac-

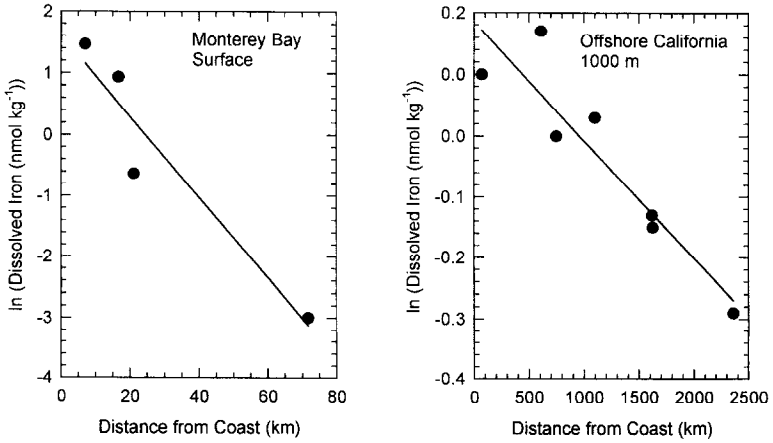

Fig. 6. Natural logarithm of dissolved iron concentrations plotted versus distance from the continental margin for a mixed layer transect offshore from Monterey Bay (a, left) and at 1000 m for a transect from central California to the central Pacific (b, right). The four shallowest samples at three stations in Monterey Bay (ONR Stations 24, 25 and 28) and one station (VERTEX V Station 1) outside the Bay reported by Martin and Gordon (1988) were used to construct the shallow transect. The deep transect was constructed using the measurement nearest to 1000 m at VERTEX V Stations 1–4, and VERTEX VI, Stations 1, 3 and 4.

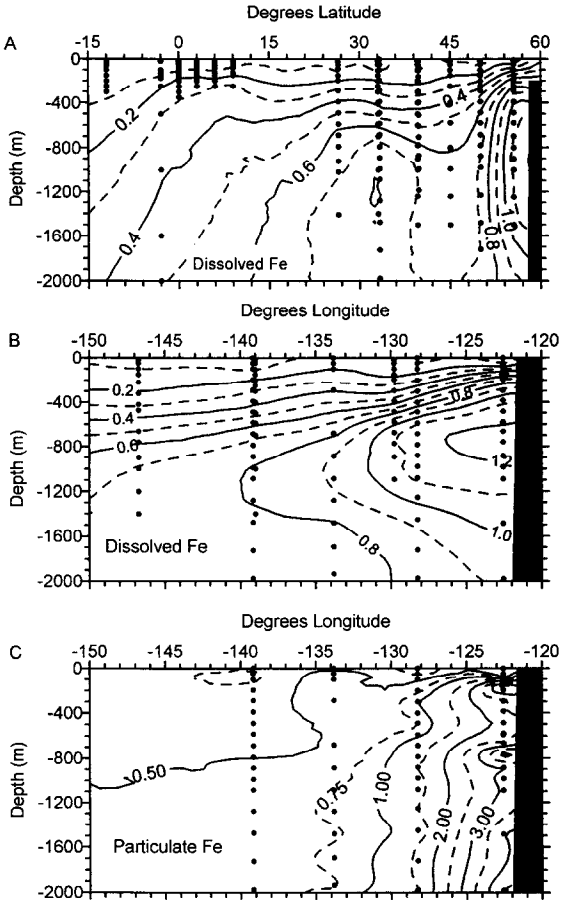

Fig. 7. Dissolved iron in a meridional section (a) near 140°W from 12°S to 55.5°N and a zonal (b) section near 33°N from 122.5°W to 146.7°W. A zonal section of particulate iron (c) near 33°N from 122.5°W to 140°W is also shown. The meridional section for dissolved iron was prepared from the four EqPac stations, five FeLine stations, VERTEX V Station 4, VERTEX VI Stations 2–5 and VERTEX VII, Stations 5–8. The zonal section of dissolved iron was constructed from the same stations used in Fig. 6b, while the VERTEX V, Stations 1–4 were used to construct the particulate iron section.

tionation for nitrate (Fig. 9a), however. There is no systematic difference between iron concentration in the Atlantic and Pacific (Fig. 9b). Concentrations of dissolved iron in the subarctic North Pacific are slightly higher than the values found in the North Atlantic. Concentrations in the equatorial South Pacific are slightly lower than the North Atlantic values.

Iron will differ from nitrate, in part, because of its tendency to be scavenged from the dissolved phase by sinking particles. Whitfield and Turner (1987) developed a scavenging index to classify the behavior of elements in the ocean with respect to removal by adsorption onto sinking particles. According to the index, iron should be strongly scavenged, as are aluminum and lead. This scavenging could act to minimize the increase of iron concentrations in deep-water due to remineralization of settling biogenic particles. Elements that are strongly scavenged, such as manganese, aluminum and lead, tend to decrease in concentration with depth and with age at a constant depth. This is just the opposite of the behavior observed for iron.

The processes that control dissolved iron concentrations must be fundamentally different than those that impact nitrate, phosphate or AOU in some important respects. Despite these differences, the vertical scale length for the increase in iron concentrations is similar to that of nitrate. This suggests that the increase in dissolved iron concentration with depth is driven by similar processes to those that regulate nitrate accumulation or the production of AOU.

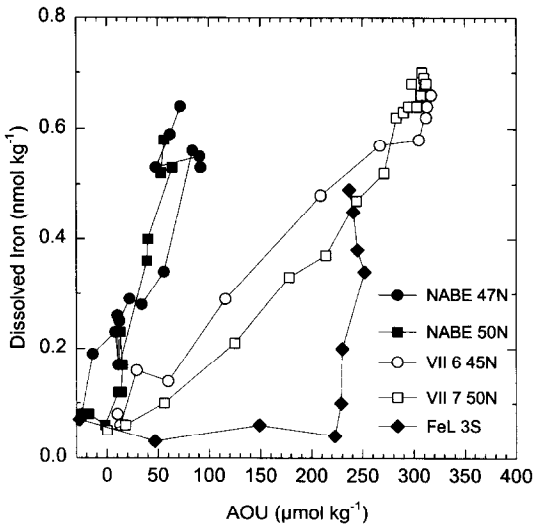

Fig. 8. Dissolved iron plotted versus apparent oxygen utilization (AOU) at NABE 47°N and 59°N stations, VERTEX VII Stations 6 and 7 and the FeLine 3°S station.

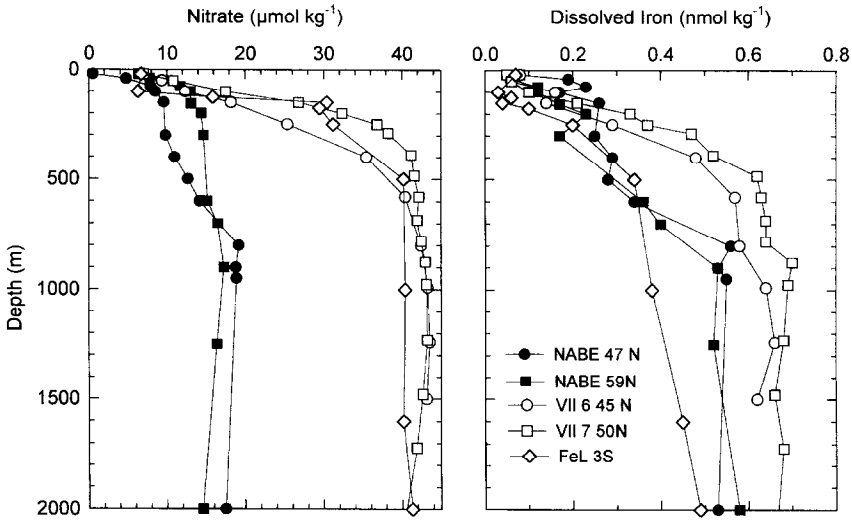

Fig. 9. Nitrate (a) and dissolved iron (b) versus depth at the same stations used in Fig. 8.

4.3. Atmospheric deposition signal

The main source of dissolved iron to surface waters in most areas of the open ocean is dissolution of iron from dust deposited at the sea surface (Duce and Tindale, 1991). Exceptions to this may occur in coastal zones or in areas of strong upwelling, such as the equatorial Pacific (Coale et al., 1996a). The iron deposited by dust can build up to detectable concentrations in the surface during periods of high dust flux and low biological production. Bruland et al. (1994) found iron concentrations at the surface in oligotrophic waters of the central Pacific gyre as high as 0.37 nmol kg^{-1}. Nitrate is extremely low in the central North Pacific, and it may limit primary production and the biological demand for iron near the surface. Dissolved iron concentrations drop rapidly with depth in this system and iron is depleted to 0.02 nmol kg^{-1} at a depth of 70 to 100 m. Nitrate concentrations begin to increase in this depth region and the chlorophyll maximum is found in the heart of the iron minimum in the euphotic zone (Bruland et al., 1994).

Wu and Luther (1994) found dissolved iron concentrations as high as 0.58 nmol kg^{-1} during summer in surface waters of the western Atlantic with very low (< 0.1 μM) NO_3^-. A strong iron minimum is again found in this system at the depth where nitrate starts to increase. A similar surface dissolved iron maximum was not present during the fall when nitrate concentrations were slightly elevated (0.5 μM). Iron concentrations were also high (0.6 nmol kg^{-1}) at the surface during winter, when strong mixing limits primary production.

Atmospheric iron deposition varies by more than 2 orders of magnitude over the geographic range that we have sampled (Duce and Tindale, 1991) and one might expect that this should be reflected in the dissolved iron concentrations, as it is for lead (Flegal and Patterson, 1983). The concentration of iron that we observed in the surface layer was uncorrelated with the flux, however. The iron deposited in surface waters is generally consumed very rapidly by phytoplankton. Apparently, iron deposited at the surface in the regions studied by Wu and Luther (1994) and by Bruland et al. (1994) was not consumed because primary production at the surface was limited by nitrate and not iron. The residence time of iron must be substantially longer in these nitrate-limited systems. Iron is rapidly depleted to concentrations that would limit production (Coale et al., 1996a; Fitzwater et al., 1996) once nitrate concentrations begin to increase at the base of the euphotic zone in these systems. We have also seen surface dissolved iron maxima (up to 0.2 nmol kg^{-1}) at several of the stations (VERTEX VI, Station 1; VERTEX VII,

Station 5) sampled by the MLML Trace Metals Laboratory where nitrate concentrations are negligible (< 0.5 μM). Thus, iron appears to accumulate to concentrations above 0.1 nmol kg^{-1} in open ocean systems only when another nutrient, such as nitrate, or light is limiting primary production.

If some of the iron deposited at the sea surface is exported with biogenic particles and then remineralized at depth, the dust deposition signal should be evident in depth integrated standing stocks of dissolved iron. To test this theory, we plotted the concentrations of iron integrated to a depth of 500 m, where most of the carbon is remineralized (Martin et al., 1987), versus the dust deposition flux of iron. A greater depth also reduced the number of stations where enough data was available. The aeolian iron flux was determined at each station using the map compiled by Duce and Tindale (1991; see also Fig. 1). The results are shown in Fig. 10. The correlation between integrated iron concentration and iron flux from the atmosphere ($R^2 = 0.34$) is significant ($P < 0.01$). The relationship between integrated iron concentrations and atmospheric iron flux is not extremely strong, however. Over the 100-fold range of fluxes that characterize most of the ocean (0.02 to 2 μmol m^{-2} yr^{-1}), the mean integrated iron concentration increases only 2-fold in the MLML data set. Furthermore, these equations account for a relatively small fraction of the variability in the integrated iron concentration. Other factors such as proximity to the coast seem to have greater impacts on the integrated stock of iron than does aeolian dust deposition.

Over the range of stations that we sampled, the data can be fit by a linear or power law relationship (Fig. 10):

$$\sum(\mathrm{Fe})\Delta Z\ (\mu\mathrm{mol\ m^{-2}}) = 86 + 0.059 J_{\mathrm{Fe}}\ (\mathrm{nmol\ m^{-2}\ y^{-1}}) \quad (1)$$

$$\sum(\mathrm{Fe})\Delta Z = 60 J_{\mathrm{Fe}}^{0.11} \quad (2)$$

The two equations predict quite different behaviors for the integrated iron concentrations when extrapolated to slightly higher dust fluxes than occurred in the regions sampled by the MLML Trace Metal Lab (Fig. 10). The linear relationship would suggest that the stock of dissolved iron would increase continuously, as the aeolian iron flux increases. The power

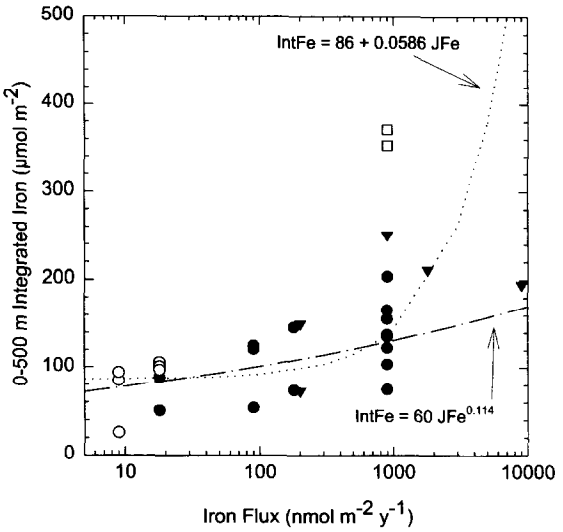

Fig. 10. The concentration of dissolved iron integrated from the surface to 500 m versus the aeolian iron flux to the sea surface. The flux was estimated from the MLML station locations (circles) and contour lines shown in Fig. 1. If a station touched a contour line it was assigned a flux equal to the contour line. If the station fell between two contour lines it was assigned a flux equal to the arithmetic average of the surrounding contour lines. At stations shown as open circles, the deepest sample was between 350 and 450 m and the last sample was used to extrapolate the integration to 500 m. The open squares are the VERTEX V Station 1 and VERTEX VII Station 8 near the continental margin and they were not used to construct the regression line. Integrated iron concentrations determined at the stations where other laboratories have measured dissolved iron concentrations that are consistent with the MLML observations (Fig. 1) are shown as triangles. Only MLML data were used to fit the lines.

equation produces an asymptotic relationship for the flux-integrated iron relationship. Such an asymptotic relationship might result if there is a solubility control on dissolved iron concentrations. Solubility control is a concept we will explore further in this paper.

The profile of iron observed in the high iron flux region of the far western Pacific by Obata et al. (1993) is more consistent with the power law relationship, than with a linear increase model (Fig. 10). Despite the high atmospheric flux, there appears to be little dissolved iron in this region. In contrast, Powell et al. (1995) report high iron concentrations (up to 10 nmol kg^{-1}) at the surface in the very high dust flux zone off North Africa, which might be more compatible with the linear relationship. Unfor-

tunately, these samples were unfiltered. We will not be able to determine whether Eq. (1) or Eq. (2) best represent the behavior of iron in the ocean until a complete dissolved iron profile is measured in a high dust flux area.

4.4. Interaction of dissolved and particulate iron

Measurements of thorium isotope distributions in the deep sea suggest that the dissolved metal concentration is controlled by a reversible equilibrium between metal on particles and in solution (Bacon and Anderson, 1982). The concentrations of dissolved iron are not well correlated with the particulate iron concentration (Fig. 11), as might result if there were an equilibrium between iron in solution and on particles. At the offshore stations, the coefficient of determination R^2 is 0.22 for a regression of dissolved versus particulate iron. A zonal section of particulate iron contoured from the data from offshore of California shows that high particulate iron extends nearly 1000 km offshore (Fig. 7c). Although both particulate and dissolved iron are high near the coast, the distribution of particulate iron along this section is considerably different from that of dissolved iron (Fig. 7b). A tongue of high dissolved iron extends offshore with maximum concentrations at depths near 1000 m, while particulate iron has highest concentrations in each profile at the maximum depth.

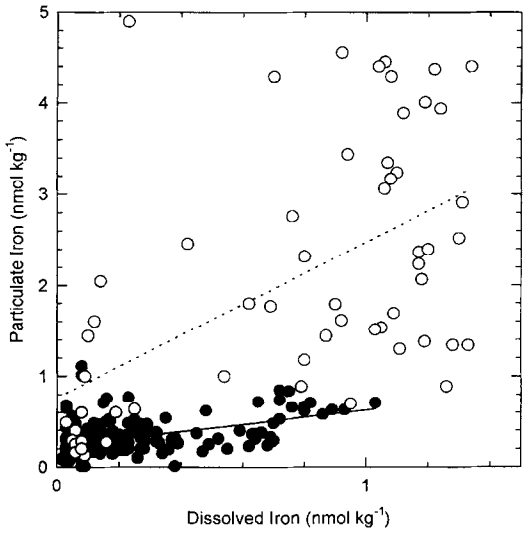

Fig. 11. Particulate iron versus dissolved iron. Data from 4 stations near the continental margin are shown as open circles (VERTEX V, Stations 1 and 2 near the California margin, VERTEX VII, Station 8 near the Alaska margin and Station 30 over the continental slope in the Ross Sea). The remaining stations are shown as closed circles. The dashed line is a least squares fit to the open circles and the solid line is a fit to the closed circles.

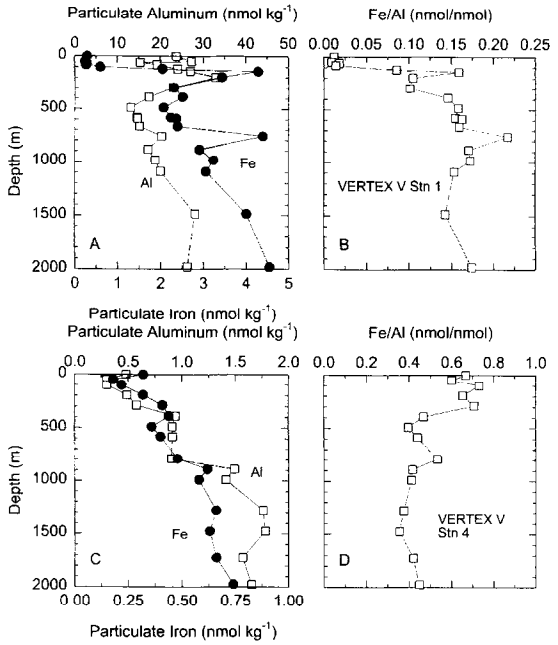

Fig. 12. Vertical profiles of particulate iron and particulate aluminum measured at VERTEX V Station 1 (a) and at Station 4 (c). Ratios of particulate iron to particulate aluminum at these stations are shown in (b) and (d), respectively.

The ratio of particulate iron to particulate aluminum at Vertex V Station 1 is shown in Fig. 12b. The Fe:Al ratio in particles averages 0.16 nmol/nmol at depths below 100 m. The deep Fe:Al ratio is close to the recent estimates of the molar Fe:Al ratios in the upper crust of 0.21 (Taylor and McLennan, 1985) and 0.19 (Wedepohl, 1995). Thus, the high particulate concentrations near the coast appear to result from crustally derived material that is being advected offshore. Griggs and Hein (1980) describe plumes of particles that are transported 100's of kilometers offshore of California. The nearly vertical isopleths of particulate iron (Fig. 7c) suggest that this material is settling fairly rapidly and that it has a different source than does dissolved iron.

The sections of dissolved and particulate iron

show that there is not a simple relationship between these constituents that is suggestive of exchange equilibrium. The data do suggest that much of the particulate iron in alumino-silicates can be removed from the solid phase and incorporated into biogenic particles that sink from surface layer. Fig. 12a shows the vertical profiles of particulate iron and particulate aluminum that were observed at Vertex V Station 1 (Martin and Gordon, 1988). The concentrations of both particulate iron and aluminum are quite high at depths below 100 m at this station, which is only 75 km off the coast. The high particulate aluminum concentrations extend to the surface, while particulate iron is nearly depleted at the surface. The ratio of particulate iron to particulate aluminum at Vertex V Station 1 drops to 0.013 above 100 m (Fig. 12b), which is significantly below the crustal ratio. The large decrease in the Fe:Al ratio near the surface, combined with high particulate aluminum concentrations, is strong evidence that solubilization of some 2 nmol kg^{-1} particulate Fe must have occurred in the euphotic zone. The solubilized particulate Fe does not appear as dissolved iron. The waters at this station have excess nitrate (> 4 μM) at the surface, while the dissolved iron concentrations are less than 0.1 nmol kg^{-1} (Fig. 5). Dissolved iron concentrations at this level would be limiting to natural populations of open ocean phytoplankton (Coale et al., 1996a; Fitzwater et al., 1996). The particulate iron may have been solubilized in order to support growth. Iron particles must be readily dissolved in the upper ocean, perhaps by photoreduction (Johnson et al., 1994; Miller et al., 1995). The remobilized iron could have been incorporated into particles that did not contain aluminum (i.e., plankton) and which were rapidly removed from the system.

Strong surface depletions, in particulate iron, such as that observed at the VERTEX V Station 1, are not as apparent at other stations in our data set. A small minimum in the particulate iron profile does appear in the nutricline at the VERTEX V Station 4 in the central Pacific (Fig. 12c). However, particulate Al concentrations in the particulate iron minimum are also low, and below our detection limit (0.36 nmol kg^{-1}). These low particulate Al values suggest that the particulate iron was not preferentially removed relative to aluminum. Bruland et al. (1994) have noted that dissolved aluminum increases in surface waters at their station in the central Pacific, which suggests that dust particles were dissolved in the euphotic zone. About half (0.35 nmol kg^{-1}) of the iron from the particles appears in the dissolved pool at their station, while the remainder (0.25 nmol kg^{-1}) appears to have been lost.

The Fe:Al molar ratio is higher than the crustal ratio at offshore stations (Fig. 12d), with surface values as high as 0.65 and decreasing to 0.4 at depth. Bruland et al. (1994) and Sherrell and Boyle (1992) also both found Fe:Al ratios in particulate matter at open ocean stations in the Pacific and Atlantic that are higher than the current estimates of the crustal ratio. The major input of iron at these stations is from marine aerosol deposition (Duce and Tindale, 1991), which has Fe:Al ratios slightly higher than the recent estimates of the crustal ratio (Duce et al., 1983). The Fe:Al ratio in particles in the central ocean gyres must be controlled by the preferential retention of particulate iron at the surface, perhaps by the plankton community. In the interior, these high Fe:Al particles mix with particles having a crustal Fe:Al ratio that are transported from the continental margin. This will decrease the Fe:Al ratio with depth.

4.5. Iron solubility and organic complexation in seawater

The relative constancy in concentration of dissolved iron at depths below 1000 m (Fig. 2b) is one of the greatest surprises in oceanic iron distributions. If iron behaved as other scavenged metals, then its concentration should decrease with depth and decrease from the Atlantic to the Pacific (Whitfield and Turner, 1987). The integrated stock of dissolved lead in the water column increases strongly as the aeolian lead flux goes up (Flegal and Patterson, 1983). In contrast to lead, the integrated stock of iron is only weakly related to that of the aeolian flux. Iron differs from scavenged metals, such as aluminum or lead, because there is a strong biological requirement for iron that leads to its uptake by living cells. Remineralization of biogenic particles must release iron, and this process must be responsible for the similarity in vertical distributions of nitrate and iron (Martin et al., 1989). As we discuss below, remineralization of iron from biogenic particles is not sufficient in the

deep-sea to maintain the observed iron concentrations against a scavenging rate equivalent to that found for metals with a similar scavenging index.

The constancy of deep-water iron concentrations suggests that removal rates of iron must decrease substantially at concentrations less than about 0.6 nmol kg^{-1}. Two mechanisms have the potential to maintain constant iron concentrations in the deep-sea. One is binding by organic ligands with a capacity to complex about 0.6 nmol kg^{-1} iron (Rue and Bruland, 1995; Wu and Luther, 1995). The second is an equilibrium between dissolved and suspended particulate iron. This equilibrium could involve relatively pure iron oxide phases or surface exchange reactions on marine particles. Concentrations of iron greater than the solubility limit or chelation capacity of seawater would be removed relatively rapidly, while concentrations at or below these values might remain in solution for much longer periods of time.

Measurements of iron–organic interactions by laboratories with a demonstrated ability to measure total iron concentrations that are consistent with our results show the presence of a strong iron binding ligand at a concentration near 0.6 nmol kg^{-1}. Rue and Bruland (1995) found two classes of iron binding ligands at stations in the central North Pacific. The strongest class of ligands had an average concentration of 0.44 nmol kg^{-1} in the upper 300 m and a range from 0.4 to 0.6 nmol kg^{-1}. Wu and Luther (1995) found iron binding ligands with similar properties in the western North Atlantic with a concentration of 0.45–0.6 nmol kg^{-1}. These ligand concentrations are very close to that required to maintain dissolved iron concentrations in the deep sea at the observed levels. Wu and Luther (1995) studied mixed layer samples only. Rue and Bruland (1995) collected samples from the entire water column. They did not find the strong iron binding ligand at depths below 500 m. However, 500 m is also the depth where total dissolved iron concentrations exceed the strong ligand concentration at their station. This would make detection of the strong ligand much more difficult, as no free ligand would be titrated by added iron (Rue and Bruland, 1995). A second, weaker ligand is present throughout the water column at concentrations near 2 nM (Rue and Bruland, 1995). This weaker ligand is present in excess of the iron concentration at all depths. Iron bound by these weaker ligands should also have a significantly reduced reactivity, unless the complex itself is scavenged onto sinking particles.

The coincidence between the strong iron binding ligand concentrations of nearly 0.6 nM in both the Pacific and Atlantic Oceans and total iron concentrations in the deep-sea near 0.6 nmol kg^{-1} does not appear to be serendipitous. The correlation may be produced by a reduction in the scavenging rate of the fraction of dissolved iron that is bound to the strong ligand. van den Berg et al. (1987) have suggested that such a mechanism accounts for the high correlation between dissolved copper concentrations and strong copper binding ligand concentration in estuaries. Whenever the copper concentration exceeds that of the strong ligand, the excess copper is preferentially scavenged. Iron binding by the strong ligand identified by Rue and Bruland (1995) may provide one mechanism to maintain the constancy of iron concentrations in deep water.

It is also possible that the apparent solubility of iron is controlled by an equilibrium with amorphous $Fe(OH)_3$. Zhu et al. (1992) have estimated a solubility for inorganic iron in seawater, with respect to $Fe(OH)_3$, of 0.66 nmol kg^{-1} at pH 8 and 25°C. They based their conclusions on a reinterpretation of the work of Byrne and Kester (1976). Sunda and Huntsman (1995) have also observed a dissolved iron solubility of 0.75 nM at a mean pH of 8.18. These solubilities are close to the value required to account for the constancy of iron in deep waters. A variety of other estimates of the solubility of inorganic iron have been obtained. Motekaitis and Martell (1987) have calculated a slightly lower solubility for $Fe(OH)_3$ in seawater of 0.15 nmol kg^{-1}. Millero et al. (1995) recently reevaluated the speciation and solubility of iron in seawater and they obtained a value of 10 nmol kg^{-1} for the solubility of inorganic iron in seawater at pH 8. These measurements have large uncertainties because of the difficulty of separating dissolved, monomeric iron from colloidal iron. The calculations also have large uncertainties because the equilibrium constants are not well constrained. Thus, the solubility of inorganic iron may impact scavenging of dissolved iron, but the uncertainty is too large to constrain the calculations.

We cannot directly verify that either of these mechanisms acts to maintain constancy of deep-water

iron concentrations. Nor can we differentiate between these mechanisms. Organic binding of iron, in particular, provides a plausible explanation for maintaining deep-water iron concentrations near 0.6 nmol kg^{-1}. We show in the next section that a simple numerical model, which incorporates an apparent iron 'solubility' near this value, provides a very good representation of the iron concentrations that we have observed throughout the ocean.

5. Dissolved Fe model

The similarity of vertical profiles of dissolved iron, nitrate and AOU suggests that they are controlled by similar processes. This implies that the major source of dissolved iron in the deep sea is release during the remineralization of organic matter. As we have shown for dissolved manganese (Johnson et al., 1996), the production rate of dissolved iron can be estimated from the change in carbon flux versus depth. The vertical flux of particulate organic carbon (POC) at a set of stations throughout the North Pacific can be fit by the equation

$$F_C = F_{100}\left(\frac{Z}{100}\right)^{-b} \quad (3)$$

where Z is the depth in m, F_{100} is the flux (mol C m^{-2} yr^{-1}) at 100 m depth and b was found to have an average value of 0.858 (Martin et al., 1987). We have adopted this equation for the work discussed here. If the Fe/C ratio of settling marine particulate organic carbon is Q (μmol Fe/mol C), then the rate of production of dissolved iron during carbon remineralization (P_{Fe}, nmol l^{-1} yr^{-1}) is

$$P_{Fe} = Q\frac{\partial F_C}{\partial Z} = \frac{b}{100^{-b}}QF_{100}Z^{-(1+b)}$$
$$= 45QF_{100}Z^{-1.858} \quad (4)$$

The rate of production of dissolved iron is controlled by the Fe/C ratio of the POC and the rate of export of POC (F_{100}).

Production of dissolved iron must be balanced by scavenging and mixing. We have assumed that scavenging removal is a first order process that occurs only when dissolved iron concentrations exceed an apparent solubility value near 0.6 nmol kg^{-1}

$$R_{Fe} = k_{Fe}[(Fe) - (Fe)_{soly}] \quad (5)$$

where (Fe) is the total dissolved iron concentration and $(Fe)_{soly}$ is the apparent solubility of dissolved iron. The scavenging rate constant is $k_{Fe} = 0$ if (Fe) is less than $(Fe)_{soly}$. The value of k_{Fe} at dissolved iron concentrations $> (Fe)_{soly}$ was treated as an adjustable parameter and determined as discussed below.

The concentration of iron is then given by the equation

$$\frac{\partial(Fe)}{\partial t} = 45QF_{100}Z^{-1.858} - k_{Fe}[(Fe) - (Fe)_{soly}] + K_Z\frac{\partial^2(Fe)}{\partial Z^2} \quad (6)$$

The last term in Eq. (6) accounts for vertical mixing of iron by eddy diffusion, and K_Z is the vertical eddy diffusion coefficient. This equation can be solved at each station to estimate the vertical profile of dissolved iron concentrations if the values of Q, F_{100}, k_{Fe}, $(Fe)_{soly}$ and K_Z are known. The export flux of carbon has been measured or estimated at a number of stations where iron has been determined (Martin et al., 1987, 1993; Johnson et al., 1996) and we will focus on those stations where these values are available. The value of $(Fe)_{soly}$ is assumed to be 0.6 nmol kg^{-1} as discussed above. The vertical eddy diffusion coefficient was set to a value of 1 cm^2 s^{-1}, which is typical of the values determined in one dimensional studies of biogeochemical processes (Munk, 1966; Craig, 1969; Gammon et al., 1982). This value also produces a reasonable vertical profile of nitrate when Eq. (6) is used to estimate nitrate remineralization with the scavenging rate constant set to zero (Fig. 13). The model eddy diffusion coefficient of 1 cm^2 s^{-1} is larger than values recently determined in deliberate tracer releases into the main thermocline (0.11 cm^2 s^{-1}; Ledwell et al., 1993) and a submarine basin (0.33 cm^2 s^{-1}; Ledwell et al., 1986). It must reflect parameterization of a variety of processes, including boundary mixing and lateral transport.

A vertical advective term would be necessary to model the distribution of conservative properties, such as temperature and salinity (Munk, 1966; Craig, 1969). The physics were parameterized only with a diffusion term in our model because it was intended to be applied in a variety of environments where

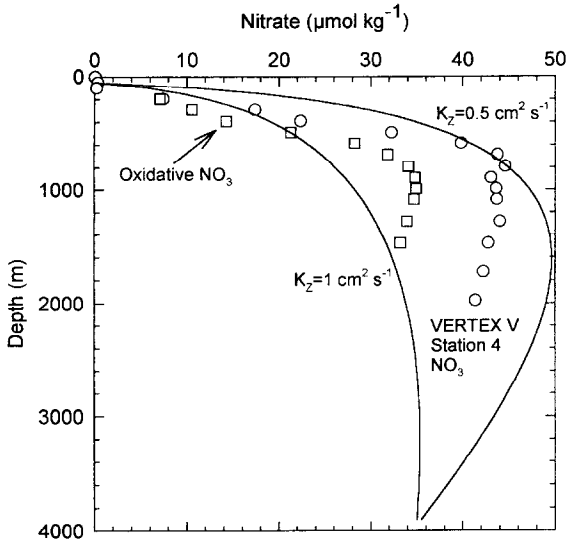

Fig. 13. A model profile of nitrate calculated with eddy diffusion coefficients of 0.5 and 1 $cm^2\ s^{-1}$. The vertical profiles of nitrate and oxidative nitrate (15×apparent oxygen utilization) at VERTEX V Station 4 in the North Pacific are shown for comparison.

there is little information on vertical velocities. A basin-scale model of ^{210}Pb, which fits the distribution of the metal observed across the North Atlantic, also includes only diffusive terms (Spencer et al., 1981).

The values of Q and k_{Fe} are only loosely constrained by measurements reported in the literature. We therefore treated them as adjustable parameters and optimized their values by a least squares fit of Eq. (6) at steady state to the vertical profile of iron observed at VERTEX VII Station 7, near Ocean Station Papa (Martin et al., 1989). Boundary conditions must also be specified to solve Eq. (6). We have assumed an upper boundary condition of (Fe) = 0.05 nmol kg^{-1} at 50 m depth. A lower boundary condition of (Fe) = 0.6 nmol kg^{-1} at 4000 m depth was used. The upper boundary condition was justified because the average mixed layer iron concentration was 0.07 nmol kg^{-1}. The lower boundary was set equal to the apparent solubility of dissolved iron at 4000 m, a depth well below that where most of the iron variability occurs.

The model results for the dissolved iron profile at VERTEX VII, Station 7 are shown in Fig. 14a. The model predicted dissolved iron profile gives an excellent fit to the observed profile. The parameter values that gave the best fit were $Q = 5$ μmol Fe/mol C and $k_{Fe} = 0.005\ yr^{-1}$ with the observed F_{100} of 2 mmol $m^{-2}\ yr^{-1}$ (MLML Trace Metals Laboratory, unpubl. data). Estimates of Q, based on laboratory experiments with open ocean phytoplankton, range from 2 to 100 μmol Fe/mol C at typical concentrations of inorganic iron (Brand, 1991; Sunda et al., 1991; Sunda and Huntsman, 1995). Martin et al. (1989) estimated an upper limit of 27 to 38 μmol Fe/mol C based on analyses of particulate matter.

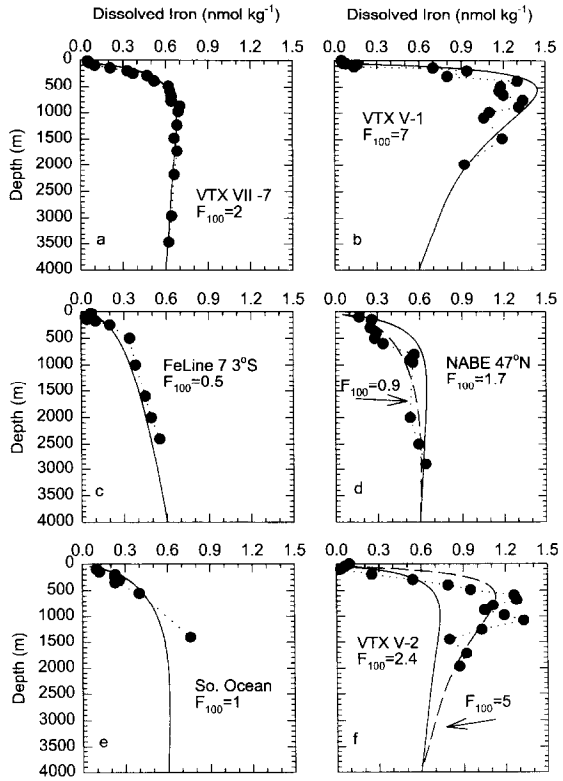

Fig. 14. Comparison of observed dissolved iron concentrations with model calculations at VERTEX VII Station 7 (Ocean Station Papa) in the North Pacific (a), FeLine 3°S, 140°W (b), VERTEX V Station 1 75 km off the California coast (c), USJGOFS NABE 47°N in the North Atlantic (d), a composite of 3 Southern Ocean stations (Drake Passage, Ross Sea Stations 30 and 98) (e), and VERTEX V Station 2 about 600 km off the California Coast (f). Model calculations with the F_{100} value estimated at each station are shown as a solid line. Best fit profiles, if substantially different than those calculated with the estimated F_{100}, are shown as dashed lines.

The best fit value for the model lies in the middle of this range and is consistent with our knowledge of oceanographic processes. Sunda and Huntsman (1995) also estimated $Q = 2.4$ μmol/mol from regressions of dissolved iron vs. phosphate in the nutricline, an approach somewhat similar to that used here.

A scavenging rate constant of 0.005 yr^{-1} is also generally consistent with observations of deep-sea metal chemistry. The residence time with respect to scavenging removal is $1/k = 200$ yr. This is reasonably close to the value of 70–140 yr estimated by Bruland et al. (1994). Their estimate was derived from the residence time of particles in the deep sea and the assumption that dissolved iron is in exchange equilibrium with the particle pool (Bacon and Anderson, 1982). The estimated residence time for aluminum in the deep sea is 150–200 yr (Orians and Bruland, 1985), which is quite similar to the value found here for iron. These elements have similar scavenging indices (Whitfield and Turner, 1987). One would expect them to have similar residence times. However, thorium also has a scavenging index similar to iron (Whitfield and Turner, 1987). The residence time of thorium in the deep-sea, with respect to scavenging, is about 30 yr (Bacon and Anderson, 1982). The difference may be due to complexation of iron by ligand 2, which exceeds the iron concentration at all depths (Rue and Bruland, 1995) and may greatly reduce its removal rate. Of course, this would imply that aluminum is heavily complexed as well.

In order to verify the generality of the model, it was used to calculate the dissolved iron concentrations at a suite of other stations from the North Atlantic to the Southern Ocean. The only geographically variable parameter in the model after Q and k_{Fe} are fixed at the values determined at VERTEX VII, Station 7 is F_{100}, the carbon export. Changes in carbon export must account for all of the horizontal variability in dissolved iron concentrations, within the context of the model developed here. The results at the FeLine 3°S station and at the VERTEX V Station 1 represent the extremes in the dissolved iron concentrations that were found at stations more than 50 km from shore. The FeLine station, in the south Pacific, has the lowest iron concentrations that were found in the upper 2000 m of the water column. The VERTEX V Station 1, which is 75 km from the California coast, has the highest dissolved iron concentrations. The export flux of carbon, F_{100}, at the FeLine 3°S station was estimated to be 0.5 mol C m^{-2} yr^{-1} (Johnson et al., 1996). It was measured to be 7 mol C m^{-2} yr^{-1} at VERTEX V Station 1 (Martin et al., 1987).

Changing only the value of F_{100} in Eq. (6) provides an excellent fit to the dissolved iron profiles observed at FeLine 3°S and at VERTEX V Station 1 (Fig. 14b, c). It appears that a 14-fold change in the export flux of carbon can account for all of the range that we have observed in dissolved iron profiles in the open ocean. Input of dissolved iron is low at the FeLine 3°S station because of the small export of carbon in the South Pacific. As a result, dissolved iron concentrations never exceeds the apparent solubility limit at this station. Scavenging does not occur and dissolved iron concentrations increase monotonically. In contrast, VERTEX V Station 1 lies at the offshore edge of the coastal upwelling zone. As a result, the export flux of carbon at VERTEX V Station 1 is 14 times higher than at the FeLine 3°S (Martin et al., 1987). The high carbon export leads to a larger iron remineralization rate. Dissolved iron concentrations build to levels near 1.4 nmol kg^{-1} before the scavenging removal rate equals the input rate. The rate of iron remineralization given by Eq. (4) decreases with depth. The remineralization rate is sufficiently small below 800 m that the dissolved iron concentration decreases. Dissolved concentrations remain in excess of the apparent solubility limit throughout the profile.

The model provides a good representation of dissolved iron concentrations throughout the ocean at other stations where we have measured iron and where estimates of F_{100} are available. Fig. 14d, e show a comparison of calculated and dissolved iron concentrations in the North Atlantic and in the Southern Ocean. The export flux of carbon (F_{100}) observed during the JGOFS North Atlantic Bloom Experiment at 47°N was 14 mmol C m^{-2} d^{-1} (Martin et al., 1993). The spring bloom carbon flux at 1000 meters is 3 times greater than the annual average carbon flux (Honjo and Manganini, 1993) so the measured F_{100} has been reduced 3-fold for an annual flux estimate of 1.7 mol C m^{-2} yr^{-1} (Johnson et al., 1996). The iron profile calculated with an

annual export flux of 1.7 mol C m^{-2} yr^{-1}, slightly overestimates the observed distribution of iron. The best fit to the North Atlantic profile was obtained with an F_{100} value of 0.9 mol C m^{-2} yr^{-1} (Fig. 14d).

The average flux of organic carbon determined over an annual cycle in the Ross Sea, at 250 m depth, was 0.5 mol C m^{-2} yr^{-1} (DeMaster et al., 1992). Extrapolating this flux to 100 m, using Eq. (3), gives an export flux of 1 mol C m^{-2} yr^{-1}. This value of F_{100} is also the best fit parameter for the dissolved iron profiles in the Southern Ocean (Fig. 14e).

The greatest discrepancy in the model predicted dissolved iron concentrations occurs at VERTEX V Station 2 (Fig. 14f). This station is over 500 km offshore and it is outside of the zone of high primary production along the ocean margin. The model fits the observed dissolved iron distributions with an F_{100} value near 5 mol C m^{-2} yr^{-1}. The observed value of F_{100} at this station is two-fold smaller (Martin et al., 1987), which leads to substantially lower predicted iron concentrations than those observed. In particular, the model using the observed F_{100} does not produce a strong mid-depth dissolved iron maximum. The dissolved iron concentrations are not anomalous at this station. The iron profile at the nearby VERTEX VI Station 1 also has a strong mid-depth maximum (Fig. 7a). The iron concentrations at 1000 m are generally compatible with the trend of the offshore gradient (Fig. 6). Several explanations may account for the discrepancy. Offshore transport of iron at depths between 500 and 1000 m may carry high concentrations of iron to this station. The residence time of dissolved iron with respect to scavenging removal is $1/k = 200$ yr. There would be sufficient time for offshore transport to produce the elevated dissolved iron concentrations seen at VERTEX V Station 2. High concentrations of particulate iron below the mixed layer at VERTEX V Station 2 (Fig. 7c) support the hypothesis of offshore transport. The coastal region off California is characterized by large meanders in the California Current with wavelengths of 300 to 500 km and filaments that extend 100's of kilometers offshore (Bernstein et al., 1977). These filaments may transport dissolved and particulate iron offshore in subsurface waters. Alternatively, the elevated dissolved iron concentrations that are centered in a narrow band at 30°N (Fig. 7b), may result from enhanced primary production and carbon export at these latitudes. Nutrients and particulate organic carbon in surface waters may be transported offshore in filaments, with the result that carbon export is enhanced in the offshore waters.

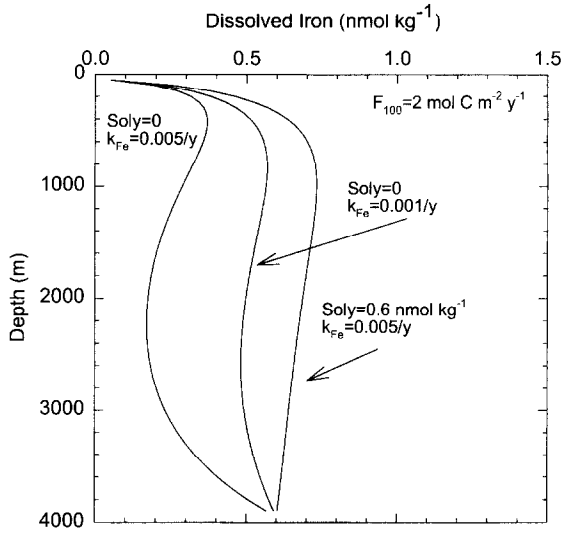

Fig. 15. Model calculation profiles of dissolved iron with the apparent solubility set to zero and scavenging rate constants of 0.005 yr^{-1} and 0.001 yr^{-1} and an F_{100} of 2 mol C m^{-2} yr^{-1}. The standard model calculation with a solubility of 0.6 nmol Fe kg^{-1} is shown for comparison.

We could not find an acceptable fit to the observed dissolved iron data unless an apparent iron solubility was included in the model. Fig. 15 shows several model calculations to illustrate this point. If scavenging is allowed to occur throughout the water column (i.e., apparent solubility = 0) and $k = 0.005$ yr^{-1}, then iron concentrations reach a shallow maximum and decrease rapidly to values much lower than seen in any data set. The decrease would be much greater if the lower boundary condition of 0.6 nmol kg^{-1} is not maintained. Decreasing the scavenging rate to 0.001 yr^{-1} improves the fit somewhat, but this implies a deep-sea residence time of 1000 yr, which is too long. Even lower scavenging rates, with no solubility term, can produce acceptable fits to observed profiles of dissolved iron. The results with no scavenging are equivalent to a solubility term that maintains iron in solution. We believe that an appar-

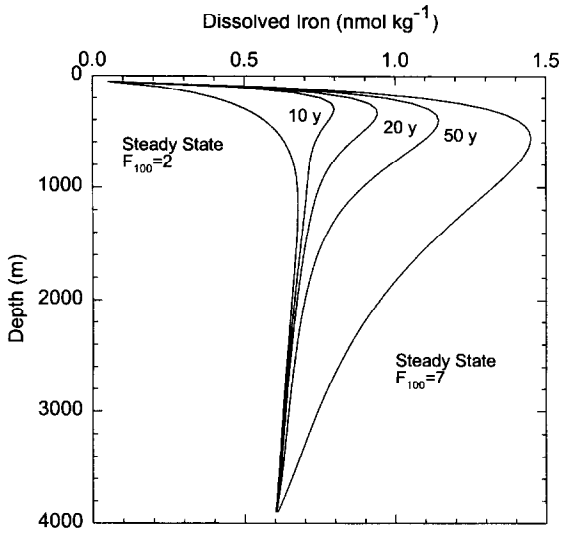

Fig. 16. Change in iron concentrations calculated at 10, 20 and 50 yr after a step change in the value of F_{100} from 2 to 7 mol C m^{-2} yr^{-1}. The steady state iron profiles for each value of F_{100} are shown as well.

ent iron solubility is the simplest explanation for the combination of a nutrient-like profile and a lack of inter-ocean fractionation.

5.1. Temporal response

The increase in iron concentration at depths below the mixed layer in the coastal zone is driven by an increase in the export flux of iron, within the context of the model. The calculations shown so far have been for steady state cases, with no change in iron over time. The residence time of water in the shelf region is limited. We have, therefore, tested the time response of the model to step increases in iron flux to assess whether it is possible for increases in carbon export over short time periods to produce the dissolved iron distributions seen in coastal regions.

Fig. 16 shows the calculated iron profiles that are obtained after increasing the value of F_{100} from 2 to 7 mol C m^{-2} yr^{-1}, beginning with an initial iron profile at steady state. Iron concentrations below the mixed layer require a decadal time scale to respond to the increased export flux of iron. After 50 yr, dissolved iron concentrations increase to levels near the steady state concentrations shown in Fig. 14b. This is rather a long time scale for water to remain in the coastal zone. The rate of increase in dissolved iron concentrations is governed quite strongly by the size of the vertical eddy diffusion coefficient used in Eq. (6). Our calculations have been based on a single value for K_Z of 1 cm^2 s^{-1}. Measurements of K_Z in the thermocline yield values closer to 0.15 cm^2 s^{-1}. Smaller values of K_Z would produce faster responses since mixing would smear the remineralized iron at a slower rate. A three-dimensional model with more realistic physics may yield a faster response time, therefore.

6. Discussion

Iron is unusual among elements with strongly depleted, nutrient-like vertical profiles. It has the smallest inter-ocean fractionation of any of these elements. There is, in fact, no systematic difference between dissolved iron concentrations in the Atlantic and Pacific Oceans. The greatest horizontal variability in dissolved iron concentration occurs not from ocean to ocean, but within single ocean basins (Fig. 7). Iron concentrations as high as 7.4 nmol kg^{-1} over the continental shelf have been observed in samples analyzed by the MLML Trace Metals Laboratory (Martin et al., 1990a,b). These high concentrations over the continental shelf must reflect input from sediments, dust and rivers. The large signal from continental sources decays away rapidly at the surface. The highest concentration that we have seen in the mixed layer at any of the open ocean stations more than 50 km from shore is 0.2 nmol kg^{-1}.

The horizontal scale lengths for iron transport away from the coast in the surface mixed layer (16 km) and at 1000 m (5000 km) differ by more than a factor of 300. The difference in the rates of iron removal at the surface and 1000 m is probably substantially greater than 300 times. Higher advection or diffusion rates in the surface layer mean that iron will be transported over a fixed distance in a lower time at the surface. The high rate of iron removal in the mixed layer is probably driven by biological uptake of iron. Our observations near the coast occur primarily in eastern boundary systems that are characterized by strong upwelling and large surface concentrations of nitrate, phosphate and sili-

cate. Primary production rates are high and iron is rapidly depleted in these systems. Dissolved iron concentrations drop to less than 1 nmol kg^{-1} within one scale length and they drop below 0.1 nmol kg^{-1} within three to four scale lengths, or 50 to 60 km. At that point, dissolved iron concentrations would be limiting to open ocean phytoplankton (Coale et al., 1996a; Fitzwater et al., 1996). Coastal phytoplankton, which have even greater iron requirements (Brand et al., 1983; Sunda and Huntsman, 1995), would be even more stressed. Nitrate concentrations are still present at concentrations > 4 μmol kg^{-1} at a distance of 75 km (VERTEX V Station 1), or 5 scale lengths offshore (Fig. 5). There is strong evidence that much of the particulate iron has been solubilized at this station. The highest chlorophyll concentrations at the VERTEX V Station 1 are 0.8 μg l^{-1} (MLML, unpublished data), which is on the low side of the chlorophyll concentrations observed off California at nitrate concentrations near 4 μM (Chavez et al., 1991). When considered in sum, all of this data suggests that the phytoplankton at the VERTEX V Station 1, only 75 km offshore, were iron limited.

Similar conclusions were reached during the Coastal Transition Zone program off the Central California coast. This study focused on the role of cross-stream jets in transporting nutrients and phytoplankton offshore. During this study, Chavez et al. (1991) found that the concentration of nitrate was often not well correlated with phytoplankton abundance. In one case, the phytoplankton population dropped dramatically after a coastal jet turned from a cross-shore to a longshore direction, although nutrient concentrations remained constant or increased. One possible explanation for this observation is that the concentration of iron dropped in this system as the offshore transport mechanism, and transport times, changed. This coastal system has all the characteristics of a high nitrate, low chlorophyll water mass in which primary production is regulated by iron limitation.

Oligotrophic systems have been described as having stratified euphotic zones, based on studies of thorium scavenging (Coale and Bruland, 1987). Primary production in the upper layer is almost completely based on recycled nutrients and there is little carbon export or metal removal. Iron may have a longer residence time at the surface in these systems, where it does not limit primary production, than in coastal systems. The major portion of the new production, carbon export and metal scavenging in oligotrophic systems is limited to a lower layer of the euphotic zone near the nitracline (Coale and Bruland, 1987). Although nitrate is increasing to high concentrations in the lower layer, dissolved iron concentrations are at a minimum in this layer (Bruland et al., 1994) due to biological uptake and scavenging. The iron concentrations in the lower region of the stratified euphotic zone are low enough (< 0.05 nmol kg^{-1}) to limit primary production (Coale et al., 1996a; Fitzwater et al., 1996). Thus, iron may regulate export production even in oligotrophic regions of the ocean.

The model that we have developed here suggests a mechanism that could account for nearly all of the variability in the open ocean iron profiles that we have observed. The model cannot account for the high dissolved iron concentrations seen near the ocean margin. Those high iron concentrations require additional sources, which are not incorporated in the model. Within the open ocean, the variability in the predicted dissolved iron concentrations could be driven solely by changes in the export of carbon. Measurements of carbon flux in the open ocean are fairly uniform, with a mean value near 1.5 mol C m^{-2} yr^{-1} (Martin et al., 1987). The relative constancy of this parameter and a high scavenging rate for dissolved iron concentrations above the ligand concentration could account for the lack of inter-ocean iron fractionation. Most of the horizontal variability in dissolved iron concentrations within the deep-sea appears to be accounted for by increases in the export of carbon as continental margins are approached. Thus, the high concentrations of dissolved iron found between 500 and 1000 m near the continental margin would not result directly from a flux from margin sediments, but from enhanced primary production and export of biogenic particles enriched in iron at the ocean margin (Martin et al., 1987). Similar conclusions were reached for dissolved manganese (Johnson et al., 1996).

Horizontal transport also plays some role regulating dissolved iron distributions, although it does not appear in the model. The carbon export measured at the VERTEX V Station 2 is insufficient to support

the observed high dissolved iron concentrations in the depth range from 500 to 1500 m. Either primary production in these regions is higher by a factor of two than believed (Martin et al., 1987), particulate organic carbon is exported offshore from coastal upwelling regions, or horizontal transport of iron in the deep-sea cannot be ignored. The presence of high particulate iron at VERTEX V Station 2 suggests that offshore transport of deep waters from the coastal margins carried the iron offshore.

The lack of inter-ocean fractionation in dissolved iron concentrations is an extremely significant indicator of the processes that control iron distributions. We believe that it is possible to simulate this behavior only by including an apparent iron solubility in the numerical model. Otherwise, iron concentrations should change significantly as the age of water in the deep-sea increases as it passes from the Atlantic to the Pacific. The mean concentration of dissolved iron that we have observed below 500 m (0.76 nmol kg^{-1}) is primarily set by the apparent solubility of iron. The apparent solubility may be controlled by the biological production of an iron binding ligand. If so, then this raises the possibility that biological processes regulate the mean dissolved iron concentration in the ocean. The mean concentration of iron is set at a point where upwelling and aeolian deposition supply just enough iron to allow phytoplankton to deplete nitrate in the bulk of the oceans mixed layer. This apparent solubility probably precludes processes such as changes in submarine hydrothermal flux from influencing the concentration of iron in the deep-sea.

Our results suggest that the aeolian deposition of iron also appears to influence the standing stock of iron in the water column. The numerical model that we have developed explicitly includes only the export flux of carbon as a geographically variable parameter. The effects of increased aeolian deposition of iron are incorporated only indirectly. The aeolian iron flux supplies iron, which can regulate primary production (Martin et al., 1994) and carbon export (Martin, 1990). This linkage is supported by the observations of Coale et al. (1996a) that primary production correlates with the integrated stock of iron within the equatorial zone of HNLC waters. The model implies, therefore, that little of an enhanced iron flux will appear as dissolved iron in the water column in regions where production is limited by another nutrient, such as nitrate.

The regions where iron regulates export production may be more widespread than previously believed. As discussed above, most of the carbon export in oligotrophic systems is limited to the lower zone of the water column (Coale and Bruland, 1987), where nitrate concentrations are increasing and iron is at a minimum (Bruland et al., 1994). Iron has a clear potential to regulate export production in these oligotrophic regions. In the coastal region offshore of California, the waters become depleted in iron before nitrate (Fig. 5), and they may represent the HNLC condition. In all of these regions, an increase in aeolian dust deposition could increase primary production and, thus, biogenic carbon and iron export. Hence, it is not surprising to see the link between integrated iron concentrations and aeolian iron input (Fig. 10).

Previous laboratory studies with single species of diatoms have suggested that particulate iron was not directly bioavailable. Photoreduction of colloidal iron can enhance iron uptake (Finden et al., 1984; Rich and Morel, 1990). The data presented here suggests that particulate iron in coastal ecosystems is mobilized and, presumably, rendered bioavailable in surface waters. The depletion in particulate iron, relative to particulate aluminum, is clearly present only at the VERTEX V Station 1. The near coastal profiles in the Gulf of Alaska (VERTEX VII, Stations 8 and 9; Martin et al., 1989) do not show similar depletions. In the Ross Sea data, there is a large depletion of iron, relative to aluminum, in the mixed layer at Station 40. There is, unfortunately, only one sample in the mixed layer at Station 40 and this observation is not repeated at other Ross Sea stations. It may be that a large input of short wavelength solar energy must occur for photoreduction of the particulate iron. This may not always occur at high latitudes with large amounts of cloud cover. Our conclusions regarding the bioavailability of particulate iron must remain somewhat tentative until these observations are repeated.

Satellite imagery has demonstrated large plumes of riverine particulate matter that are transported at least 100 km offshore of California (Griggs and Hein, 1980). These plumes may represent an important source of iron to the coastal phytoplankton

community. Up to 2 nmol kg^{-1} of particulate iron appear to have been solubilized and probably consumed in the euphotic zone at the VERTEX V Station 1 (Fig. 12a). We have argued above that the outer regions of the coastal ocean may be iron limited. Processes that change the particulate iron flux to the ocean may have an impact on coastal productivity, therefore. For example, reductions in river flow and sediment load due to construction of dams can greatly reduce the flux of particulate iron to the coastal zone. In a study of rivers in the southeastern US, about 95% of the sediment eroded in upland regions is trapped due to extensive impoundments (Trimble, 1975). Regional sediment yields are 10 times smaller along the central and southern California coast than in northern California (Griggs and Hein, 1980). This reduction is due in part to the large number of dams and water-diversion projects in central and southern California. Large reductions in secondary production off the California coast have been identified over the past 20 to 40 yr (Roemmich and McGowan, 1995). It is possible that this may be linked to a reduced flux of bioavailable particulate iron due to the contemporaneous construction of dams and other impoundments in this region. If so, then this impact could be quite widespread, as humans now consume about 17% of the global runoff (Postel et al., 1996).

7. Major questions

What are the major questions regarding iron chemistry in the deep-sea that remain to be answered? We have a very limited picture of iron chemistry that is obscured by the difficulties in comparing measurements between laboratories. As we have shown here, there appears to be substantial agreement among the measurements of five laboratories. All of these laboratories have produced iron profiles with a nutrient-like shape that converge on concentrations near 0.6 nmol kg^{-1} in the deep-sea. The numerical model that we present here suggests that these dissolved iron profiles should be typical of most of the ocean. We believe that the work of these laboratories provides substantial evidence that the major features of this model are correct. Our confidence in future measurements of dissolved iron will be greatly enhanced if the standards for dissolved iron at < 1 nmol kg^{-1} were available. In addition, laboratories involved in these studies should make an attempt to measure profiles of dissolved iron in the open ocean in regions where interlaboratory agreement has been demonstrated. Such interlaboratory agreement is necessary before much confidence can be placed in anomalously high dissolved iron concentrations measured in the marine environment.

Despite the agreement of five laboratories on the general features of the iron profile, there are no measurements in many areas of the ocean, there are few time series measurements (Wu and Luther, 1994) and few detailed transects of iron across coastal boundaries (Martin and Gordon, 1988). Efforts to measure detailed dissolved iron profiles in areas of very high aeolian iron flux should be made. Measurements of dissolved iron profiles in areas of high carbon export, in conjunction with estimates of the export flux, also need to be made. All of these measurements would be of great importance to help test the assumptions inherent in the model that we have developed.

The data summarized here suggest that iron plays a more extensive role in regulating carbon export from the ocean than previously believed. This regulation appears to occur in at least one coastal location and within the nutricline at the base of the euphotic zone in oligotrophic waters. All of our observations to date (Coale et al., 1996a; Coale et al., 1996b; Fitzwater et al., 1996) suggest that iron regulation of productivity in the open ocean occurs at concentrations < 0.2 nmol kg^{-1}. Very small changes in iron concentration or iron flux (with no actual concentration change) may be responsible for biological patchiness under these conditions (Young et al., 1991). These ideas can be tested by a combination of careful measurements of dissolved iron and concurrent incubations of seawater in paired control and iron-spiked treatments. These experiments should focus on the impacts of iron concentration changes at levels near the ambient. The role of particulate iron as a source of bioavailable iron needs to be carefully studied with a mixture of both field observations and incubation experiments. These experiments should focus carefully on processes such as photoreduction of iron and production of iron binding ligands.

The solubilizing effect of organic complexation appears to play a critical role in setting the mean

concentration of dissolved iron in the deep sea. The deep sea concentration in turn must control the upward flux of iron to the euphotic zone as well. It is essential that we learn more about the role of organic complexation in regulating the physical chemistry of dissolved iron at sub-nanomolar concentrations and subsequent effect on iron retention in the deep-sea. Very careful titrations of deep samples, where the concentrations of dissolved iron may exceed the strong ligand concentration need to be performed to assess the presence of strong iron binding ligands.

The role of iron in regulating coastal productivity needs to be carefully examined. We cannot currently answer such simple questions as whether or not iron is elevated in upwelling zones. The potential for particulate iron to be rendered bioavailable in coastal zones should also be examined more closely. The role of iron photochemistry in making particulate iron bioavailable needs to be considered in conjunction with this question.

Acknowledgements

This work was supported by NSF Grants OCE9202109 and OCE9217518 and ONR Grants N00014-89-J-1010 and N00014-84-C-0619. This data was primarily collected during projects supervised by the late John Martin, and it was his perseverance that allowed a data set of this quality to be developed. The assistance of Steve Fitzwater, Craig Hunter, Sara Tanner, Ginger Elrod and Jocelyn Nowicki is greatfully acknowledged. The numerical model is available at http://color.mlml.calstate.edu/www/data/ as an Excel 5.0 spreadsheet.

References

Bacon, M.P., Anderson, R.F., 1982. Distribution of thorium isotopes between dissolved and particulate forms in the deep sea. J. Geophys. Res. 87, 2045–2056.

Bernstein, R.L., Breaker, L., Whritner, R., 1977. California Current eddy formation: Ship, air, and satellite results. Science 195, 353–359.

Boyle, E.A., Sclater, F.R., Edmond, J.M., 1977. The distribution of dissolved copper in the Pacific. Earth Planet. Sci. Lett. 37, 38–54.

Brand, L.E., 1991. Minimum iron requirements of marine phytoplankton and the implications for biogeochemical control of new production. Limnol. Oceanogr. 36, 1756–1771.

Brand, L.E., Sunda, W.G., Guillard, R.R.L., 1983. Limitation of marine phytoplankton reproduction rates by zinc, manganese and iron. Limnol. Oceanogr. 28, 1182–1198.

Broecker, W.S., Peng, T.-H., 1982. Tracers in the Sea. ELDIGO Press, Columbia University, Palisades, NY.

Bruland, K.W., Franks, R.P., 1983. Mn, Ni, Cu, Zn and Cd in the western North Atlantic. In: Wong, C.S., Boyle, E., Bruland, K.W., Burton J.D., Goldberg, E.D. (Eds.), Trace Metals in Sea Water. Plenum, New York, pp. 395–414.

Bruland, K.W., Franks, R.P., Knauer, G.A., Martin, J.H., 1979. Sampling and analytical methods for the determination of copper, cadmium, zinc and nickel at the nanogram per liter level in sea water. Anal. Chim. Acta 105, 223–245.

Bruland, K.W., Donat, J.R., Hutchins, D.A., 1991. Interactive influences of bioactive trace metals on biological production in oceanic waters. Limnol. Oceanogr. 36, 1555–1577.

Bruland, K.W., Orians, K.J., Cowen, J.P., 1994. Reactive trace metals in the stratified central North Pacific. Geochim. Cosmochim. Acta 58, 3171–3182.

Byrne, R.H., Kester, D.R., 1976. Solubility of hydrous ferric oxide and iron speciation in seawater. Mar. Chem. 4, 255–274.

Chavez, F.C., Barber, R.T., Kosro, P.M., Huyer, A., Ramp, S.R., Stanton, T.P., de Mendiola, B.R., 1991. Horizontal transport and the distribution of nutrients in the coastal transition zone off Northern California: Effects on primary production, phytoplankton biomass and species composition. J. Geophys. Res. 96, 14833–14848.

Coale, K.H., 1991. The effects of iron, manganese, copper and zinc on primary production and biomass in plankton of the subarctic Pacific. Limnol. Oceanogr. 36, 1851–1864.

Coale, K.H., Bruland, K.W., 1987. Oceanic stratified euphotic zone as elucidated by ^{234}Th:^{238}U disequilibria. Limnol. Oceanogr. 32, 189–200.

Coale, K.H., Fitzwater, S.E., Gordon, R.M., Johnson, K.S., Barber, R.T., 1996a. Control of community growth and export production by upwelled iron the equatorial Pacific Ocean. Nature 379, 621–624.

Coale, K.H., Johnson, K.S., Fitzwater, S.E., Gordon, R.M., Tanner, S., Chavez, F.P., Ferioli, L., Sakamoto, C., Rogers, P., Millero, F., Steinberg, P., Nightingale, P., Cooper, D., Cochlan, W.P., Landry, M.R., Constantinou, J., Rollwagen, G., Trasvina, A., Kudela, R., 1996b. A massive phytoplankton blooms induced by an ecosystem-scale iron fertilization experiment in the equatorial Pacific Ocean. Nature 383, 495–501.

Craig, H., 1969. Abyssal carbon and radiocarbon in the Pacific. J. Geophys. Res. 74, 5491–5506.

de Baar, H.J.W., 1994. Von Liebig's law of the minimum and plankton ecology (1899–1991). Prog. Oceanogr. 33, 347–386.

de Baar, H.J.W., Buma, A.G.J., Nolting, R.F., Cadee, G.C., Jacques, G., Treguer, P.J., 1990. On iron limitation of the Southern Ocean: Experimental observations in the Weddell and Scotia Seas. Mar. Ecol. Prog. Ser. 65, 105–122.

DeMaster, D.J., Dunbar, R.B., Gordon, L.I., Leventer, A.R., Morrison, J.M., Nelson, D.M., Nittrouer, C.A., Smith, W.O.

Jr., 1992. Cycling and accumulation of biogenic silica and organic matter in high-latitude environments: the Ross Sea. Oceanography 5, 146–153.

Duce, R.A., Tindale, N.W., 1991. Atmospheric transport of iron and its deposition in the ocean. Limnol. Oceanogr. 36, 1715–1726.

Duce, R.A., Arimoto, R., Ray, B.J., Unni, C.K., Harder, P.J., 1983. Atmospheric trace elements at Enewetak Atoll: 1, concentrations, sources and temporal variability. J. Geophys. Res. 88, 5321–5342.

Eggiman, D.W., Betzer, P.W., 1976. Decomposition and analysis of refractory suspended materials. Anal. Chem. 48, 866–890.

Finden, D.A.S., Tipping, E., Jaworski, G.H.M., Reynolds, C.S., 1984. Light-induced reduction of natural iron(III) oxide and its relevance to phytoplankton. Nature 309, 783–784.

Fitzwater, S.E., Coale, K.H., Gordon, R.M., Johnson, K.S., Ondrusek, M.E., 1996. Iron deficiency and phytoplankton growth in the Equatorial Pacific. Deep-Sea Res. II 43, 995–1015.

Flegal, A.R., Patterson, C.C., 1983. Vertical concentration of profiles of lead in the Central Pacific at 15°N and 20°S. Earth Planet. Sci. Lett. 64, 19–32.

Gammon, R.H., Cline, J., Wisegarver, D., 1982. Chlorofluoromethanes in the northeast Pacific Ocean: Measured vertical distributions and application as transient tracers of upper ocean mixing. J. Geophys. Res. 87, 9441–9454.

Geider, R.J., La Roche, J.L., 1994. The role of iron in phytoplankton photosynthesis, and the potential for iron-limitation of primary production in the sea. Photosyn. Res. 39, 275–301.

Gordon, R.M., Johnson, K.S., Coale, K.H., submitted.Behavior of iron and other trace elements in IronEx I and PlumEx. Deep-Sea Res.

Griggs, G.B., Hein, J.R., 1980. Sources, dispersal and clay mineral composition of fine-grained sediment off central and northern California. J. Geol. 88, 541–566.

Honjo, S., Manganini, S.J., 1993. Annual biogenic particle fluxes to the interior of the North Atlantic Ocean; studied at 34°N 21°W and 48°N 21°W. Deep-Sea Res. 40, 587–607.

Hutchins, D.A., 1995. Iron and the marine phytoplankton community. In: Chapman, D., Round, F. (Eds.), Progress in Phycological Research, Vol. 11. Biopress Ltd., pp. 1–49.

Johnson, K.S., Coale, K.H., Elrod, V.A., Tindale, N.W., 1994. Iron photochemistry in seawater from the equatorial Pacific. Mar. Chem. 46, 319–334.

Johnson, K.S., Coale, K.H., Berelson, W.M., Gordon, R.M., 1996. On the formation of the manganese maximum in the oxygen minimum. Geochim. Cosmochim. Acta 60, 1291–1299.

Kumar, N., Anderson, R.F., Mortlock, R.A., Froelich, P.N., Kubik, P., Dittrich-Hannen, B., Suter, M., 1995. Increased biological productivity and export production in the glacial Southern Ocean. Nature 378, 675–680.

Landing, W.M., Bruland, K.W., 1987. The contrasting biogeochemistry of iron and manganese in the Pacific Ocean. Geochim. Cosmochim. Acta 51, 29–43.

Landing, W.M., Cutter, G.A., Dalziel, J.A., Flegal, A.R., Powell, R.T., Schmidt, D., Shiller, A., Statham, P., Westerlund, S., Reising, J., 1995. Analytical intercomparison results from the 1990 Intergovernmental Oceanographic Commission open-ocean basclinc survcy for tracc metals: Atlantic Ocean. Mar. Chem. 49, 243–252.

Ledwell, J.R., Watson, A.J., Broecker, W.S., 1986. A deliberate tracer experiment in Santa Monica Basin. Nature 323, 322–324.

Ledwell, J.R., Watson, A.J., Law, C.S., 1993. Evidence for slow mixing across the pycnocline from an open-ocean tracer-release experiment. Nature 364, 701–703.

Martin, J.H., Fitzwater, S.E., 1988. Iron deficiency limits phytoplankton growth in the north–east Pacific subarctic. Nature 331, 341–343.

Martin, J.H., Gordon, R.M., 1988. Northeast Pacific iron distributions in relation to phytoplankton productivity. Deep-Sea Res. 35, 177–196.

Martin, J.H., Knauer, G.A., Karl, D.M., Broenkow, W.W., 1987. VERTEX: Carbon cycling in the northeast Pacific. Deep-Sea Res. 34, 267–285.

Martin, J.H., Gordon, R.M., Fitzwater, S., Broenkow, W.W., 1989. VERTEX: Phytoplankton/iron studies in the Gulf of Alaska. Deep-Sea Res. 36, 649–680.

Martin, J.H., Fitzwater, S.E., Gordon, R.M., 1990a. Iron deficiency limits phytoplankton growth in Antarctic waters. Global Biogeochem. Cycl. 4, 5–12.

Martin, J.H., Gordon, R.M., Fitzwater, S.E., 1990b. Iron in Antarctic waters. Nature 345, 156–158.

Martin, J.H., Fitzwater, S.E., Gordon, R.M., Hunter, C.N., Tanner, S.J., 1993. Iron, primary production, and carbon–nitrogen flux studies during the JGOFS North Atlantic bloom experiment. Deep-Sea Res. 40, 115–134.

Martin, J.H., Coale, K.H., Johnson, K.S., Fitzwater, S.E., Gordon, R.M., Tanner, S.J., Hunter, C.N., Elrod, V.A., Nowicki, J.L., Coley, T.L., Barber, R.T., Lindley, S., Watson, A.J., Van Scoy, K., Law, C.S., Liddicoat, M.I., Ling, R., Stanton, T., Stockel, J., Collins, C., Anderson, A., Bidigare, R., Ondrusek, M., Latasa, M., Millero, F.J., Lee, K., Yao, W., Zhang, J.Z., Friederich, G., Sakamoto, C., Chavez, F., Buck, K., Kolber, Z., Greene, R., Falkowski, P., Chisholm, S.W., Hoge, F., Swift, R., Yungel, J., Turner, S., Nightingale, P., Hatton, A., Liss, P., Tindale, N.W., 1994. Testing the iron hypothesis in ecosystems of the Equatorial Pacific Ocean. Nature 371, 123–129.

Miller, W.L., King, D.W., Lin, J., Kester, D.R., 1995. Photochemical redox cycling of iron in coastal seawater. Mar. Chem. 50, 63–77.

Millero, F.J., Yao, W., Aicher, J., 1995. The speciation of Fe(II) and Fe(III) in natural waters. Mar. Chem. 50, 21–39.

Motekaitis, R.J., Martell, A.E., 1987. Speciation of metals in the oceans. I. Inorganic complexes in seawater, and influence of added chelating agents. Mar. Chem. 21, 101–116.

Munk, W.H., 1966. Abyssal recipes. Deep-Sea Res. 13, 707–730.

Obata, H., Karatani, H., Nakayama, E., 1993. Automated determination of iron in seawater by chelating resin concentration and chemiluminescence detection. Anal. Chem. 65, 1524–1528.

Orians, K.J., Bruland, K.W., 1985. Dissolved aluminium in the central North Pacific. Nature 316, 427–429.

Postel, S.L., Daily, G.C., Ehrlich, P.R., 1996. Human appropriation of renewable fresh water. Science 271, 785–788.

Powell, R.T., King, D.W., Landing, W.M., 1995. Iron distributions in surface waters of the south Atlantic. Mar. Chem. 50, 13–20.

Rich, H.W., Morel, F.M.M., 1990. Availability of well-defined iron colloids to the marine diatom *Thalassiosira weisflogii*. Limnol. Oceanogr. 35, 652–662.

Roemmich, D., McGowan, J., 1995. Climatic warming and the decline of zooplankton in the California Current. Science 267, 1324–1326.

Rue, E.L., Bruland, K.W., 1995. Complexation of iron(III) by natural organic ligands in the Central North Pacific as determined by a new competitive ligand equilibration/adsorptive cathodic stripping voltammetric method. Mar. Chem. 50, 117–138.

Sherrell, R.M., Boyle, E.A., 1992. The trace metal composition of suspended particles in the oceanic water column near Bermuda. Earth Planet. Sci. Lett. 111, 155–174.

Spencer, D.W., Bacon, M.P., Brewer, P.G., 1981. Models of the distribution of ^{210}Pb in a section across the North Equatorial Pacific Ocean. J. Mar. Res. 39, 119–138.

Sunda, W.G., Huntsman, S.A., 1995. Iron uptake and growth limitation in oceanic and coastal phytoplankton. Mar. Chem. 50, 189–206.

Sunda, W.G., Swift, D.G., Huntsman, S.A., 1991. Low iron requirement for growth in oceanic phytoplankton. Nature 351, 55–57.

Takeda, S., Kamatani, A., Kawanobe, K., 1995. Effects of nitrogen and iron enrichments on phytoplankton communities in the northwestern Indian Ocean. Mar. Chem. 50, 229–241.

Taylor, S.R., McLennan, S.M., 1985. The Continental Crust: Its Composition and Evolution. Blackwell, Oxford.

Trimble, S.W., 1975. Denudation studies: Can we assume stream steady state?. Science 188, 1207–1208.

van den Berg, C.M.G., Merks, A.G.A., Duursma, E.K., 1987. Organic complexation and its control of the dissolved concentrations of copper and zinc in the Scheldt Estuary. Est. Coast. Shelf Sci. 24, 785–797.

Wedepohl, K.H., 1995. The composition of the continental crust. Geochim. Cosmochim. Acta 59, 1217–1232.

Wells, M.L., Price, N.M., Bruland, K.W., 1995. Iron chemistry in seawater and its relationship to phytoplankton: A workshop report. Mar. Chem. 48, 157–182.

Whitfield, M., Turner, D.R., 1987. The role of particles in regulating the composition of seawater. In: Stumm, W. (Ed.), Aquatic Surface Chemistry. Wiley, New York, pp. 457–493.

Wu, J., Luther, G.W., 1994. Size-fractionated iron concentrations in the water column of the western North Atlantic Ocean. Limnol. Oceanogr. 39, 1119–1129.

Wu, J., Luther, G.W., 1995. Complexation of Fe(III) by natural organic ligands in the Northwest Atlantic Ocean by a competitive ligand equilibration method and kinetic approach. Mar. Chem. 50, 159–177.

Young, R.W., Carder, K.L., Betzer, P.R., Costello, D.K., Duce, R.A., DiTullio, G.R., Tindale, N.W., Laws, E.A., Uematsu, M., Merrill, J.T., Feeley, R.A., 1991. Atmospheric iron inputs and primary productivity: Phytoplankton responses in the North Pacific. Global Biogeochem. Cycl. 5, 119–134.

Zhu, Z., Prospero, J.M., Millero, F.M., Savoie, D.L., Brass, G.W., 1992. The solubility of ferric iron in marine mineral aerosol solutions at ambient relative humidities. Mar. Chem. 38, 91–107.